Seismic Assessment of Itanagar City, Arunachal Pradesh, India: ELGRA Studies Incorporating Spatially Variable Subsurface Stratification derived from Active MASW Survey

Short Title: **Seismic Assessment of Itanagar City using ELGRA and MASW Studies**

Aditya Kumar Anshu[1], Arindam Dey[2], Shiv Shankar Kumar[3], Jumrik Taipodia[4]

[1]Aditya Kumar Anshu
Research Scholar, Department of Civil Engineering, National Institute of Technology, Arunachal Pradesh 791113, India. ORCID No.: 0000-0002-9493-0166
Email: aditya.phd20@nitap.ac.in

[2]Arindam Dey*
Associate Professor, Department of Civil Engineering, Indian Institute of Technology Guwahati, Assam, India. ORCID No.: 0000-0001-7007-2729. Contact No.: +918011002709
Email: arindam.dey@iitg.ac.in

[3]Shiv Shankar Kumar
Assistant Professor, Department of Civil Engineering, National Institute of Technology Patna, Patna 800005, India. ORCID No.: 0000-0002-1751-8020
Email: k.shiv.ce@nitp.ac.in

[4]Jumrik Taipodia
Assistant Professor, Department of Civil Engineering, National Institute of Technology, Arunachal Pradesh 791113, India. ORCID No.:0000-0001-8943-8014.
Email: jumrik@nitap.ac.in

* Corresponding author

Funding: No funding has been received for this study

Compliance with Ethical Standards

Conflict of Interest: No potential conflict of interest was reported by the authors.

Ethical Approval: This article does not contain any studies with human participants or animals performed by any of the authors.

Informed Consent: For this type of study, formal consent is not required.

Seismic Assessment of Itanagar City, Arunachal Pradesh, India: ELGRA Studies Incorporating Spatially Variable Subsurface Stratification derived from Active MASW Survey

Abstract: This study investigates the seismic response of 22 selected locations across the Itanagar region using equivalent linear ground response analysis (ELGRA). The analysis incorporates shear wave velocity data obtained from active multichannel analysis of surface waves (MASW) field tests as input parameters for ELGRA. Four distinct acceleration-time histories were used as strong motion inputs to consider a wide range of peak bedrock acceleration (PBA) ranging from 0.026g to 0.82g. The results reveal the significant spatial variability in ground response parameters such as peak ground acceleration (PGA), amplification factor, displacement, shear strain, spectral acceleration (SA) and shear stress ratio profiles. The surface PGA in the Itanagar city is found to be within the range 0.064g to 1.71g along with the amplification factors varying between varied in between 0.4 to 11. For motions with PBA more than 0.343g, few locations in the city exhibited deamplification as well, thereby lowering down the influence of the higher seismic energy imparted by the chosen motion. The study successfully highlights the variability of peak spectral acceleration (PSA) in the region, especially identifying the locations manifesting higher magnitudes of PSA. The identified period bandwidths at different locations of high PSA (0.05-0.2 s for lower PBA motions and 0.2-0.4 for higher PBA motions) indicate the potential vulnerability of infrastructures with approximately similar natural periods. The variability of spectral acceleration within the region corresponding to the periods of 0.1 s, 0.3 s, and 0.5 s clearly demarcated the locations where buildings with specific heights would be subjected to higher seismic forces. This study provides valuable insights into the seismic response of the Itanagar region, highlighting the importance of site-specific geological conditions in influencing ground motion amplification. The findings of this analysis can be efficiently utilized for the development of seismic resilient structures and to enhance the seismic risk management strategies in the region.

Keywords: Equivalent linear ground response analysis (ELGRA); MASW; Seismic assessment; Ground response parameters; PGA and Amplification factor; Spectral ratio; Spatial variability.

1. Introduction

Over the years, earthquake events have adequately demonstrated the effect of site amplification and the resulting damages inflicted on the built environment and even leading to their collapse. The occurrence of earthquake causes regional ground shaking, yet exhibiting significantly varying characteristics of wave amplifications (manifested in terms of altered frequency and amplitudes with respect to the input strong motion) recorded in the localized areas due to the variation in the local site conditions. Several earthquakes over the years have demonstrated the devastating impact of seismic activity, underscoring the necessity for detailed seismic hazard assessments, among which Shillong earthquake (1897), Assam earthquake (1950), Guerrero earthquake (1985), Spitak earthquake (1988), Loma Prieta earthquake (1989), Uttarkashi earthquake (1991), Kobe earthquake (1995), Kocaeli earthquake (1999), Sikkim earthquake (2011), Nepal earthquake (2015), Kahramanmaras earthquake (2023) to name a few. Even though each of these earthquakes released enormous amount of energy in the soil overburden over a large region, yet the damages in the ground structures surrounding the epicentre is quite diverse, and is primarily guided by the local soil geology and existing compositions. Thus, it becomes imperative to conduct site-specific Seismic Ground Response Studies (SGRS) to identify the local site effects on the amplification of seismic waves that would, in turn, consequently help to design seismically resilient structures in a locality and establish the corresponding design parameters (Fayjaloun *et al.* 2021; Sabetta *et al.* 2023). There is reasonable amount of such studies that has been conducted on the Indian territory as well as around the world in order to assess the influence of local subsurface stratification on ground response. Govindaraju *et al.* (2004) have performed SGRS for Ahmedabad city, Gujarat, using equivalent linear approach with SHAKE91 (Idriss and Sun 1992), wherein the shear wave velocity (V_s) was estimated from the available correlations with SPT-N, as recommended by Japan Road Association (Lee 1992). In a similar manner of utilizing established correlations to determine V_s from SPT-N values, Phanikanth *et al.* (2011) resorted to DEEPSOIL program to conduct ground response studies of Mumbai city using equivalent linear approach. Similar approach was adopted by Anbazhagan *et al.* (2013) to perform SGRS of Lucknow city, and based on average shear wave velocity for 30 m depth (V_s^{30}), the region was classified into site classes C and D (NEHRP 2020) with the amplification factor ranging in 3.5-5.54. In an identical pattern, Puri *et al*. (2018) also used SPT-based correlations to assess V_s^{30} and utilized it as input in the DEEPSOIL software for conducting ground response studies of Haryana state, India. A similar exercise was carried out by Naik and Choudhury (2013) to assess the ground response of Panjim City, Goa, wherein significant variation in the amplification factors was illustrated as an impact of local soil characteristics when subjected to strong motions with varying peak ground accelerations (PGA) ranging from 0.17g to 0.24g.

It is quite evident that as the stiffness changes with depth and confining pressure (Kumar *et al.* 2020), depending on the subsurface conditions, the shear wave velocity will also differ throughout the depth. In such scenario, instead of sparse borehole-based point assessments, dense seismic arrays (Guzel *et al.* 2020) or Multichannel Analysis of Seismic Wave (MASW) techniques (Taipodia *et al.* 2020) can provide effective means to make a continuous profiling of the subsurface shear wave velocity. It is important to capture the variability as well as establish the uncertainty in the subsurface characteristics to the best possible extent while conducting ground response analysis studies (Rathje *et al*. 2010; Jiang *et al.* 2022). In absence of borehole-based findings, it has been successfully illustrated in research studies that subsurface identification can be successfully achieved through wave propagation techniques such as seismic refraction and MASW surveys (Gazetas 1982; Taipodia *et al.* 2018). Such techniques are amply effective in exploring the layered soil deposits having changing stiffness, and several researchers have made successful use of it in microzonation studies. The Department of Science and Technology (DST), Government of India, had initiated microzonation of 63 cities at the national level (Bansal and Vandana 2007), some of which have been completed while others are still in progress. As an initial experiment, seismic hazard analysis and microzonation studies were conducted for Jabalpur city, Madhya Pradesh (Rao *et al.* 2011) [19]. Several other cities have also been included under this umbrella of studies such as Sikkim (Nath *et al.* 2009) [20], Mumbai (Mhaske and Choudhury 2011), Delhi (Rao and Rathod 2014), Guwahati (Basu *et al.* 2019), Ahmedabad (Sairam *et al.* 2018), Bhuj (Mohan *et al.* 2024), Dehradun (Mahajan *et al.* 2007), Lucknow (Kumar *et al.* 2013) and Chennai (Boominathan *et al.* 2008; Maheswari *et al.* 2010). While emphasizing upon the importance of soil geology in SGRS, Mahajan *et al.* (2007) resorted to MASW survey in Dehradun city and provided the subsurface stratification through the variations of shear wave velocity with depth. Based on the SGRS using SHAKE2000 (Ordonez 2011), the amplification factor for the seismic wave in Dehradun city area was reported to be in the range of 1-4. A similar approach of conducting SGRS studies for Bengaluru city, India, was adopted by Anbazhagan and Sitharam (2008), in which the subsurface identification using MASW surveys that categorized the region into Site Classes C and D. Based on MASW-based shear wave velocity profiling of Chennai city, India, Maheshwari *et al.* (2008) employed equivalent linear and nonlinear approaches by SHAKE91 and Flac3D, respectively, to conduct SGRS studies. Aided by shear-wave velocity profiling obtained from MASW, the dynamic response of soil can be effectively assessed using equivalent linear or nonlinear approaches of ground response analysis (Basu *et al.* 2017; Kumar *et al.* 2018; Basu *et al.* 2019; Dey *et al.* 2021; Hashash *et al.* 2024; Anshu *et al.* 2024). The nonlinear approach of conducting ground response analyses is better suited to capture the hysteretic response of the soil owing to the incorporation of modulus degradation and strain-dependent damping ratio. Even though this approach is a better candidate to accurately assess the evolution of strains and deformation with cycles of loading, yet the execution of nonlinear ground response analysis requires more advanced computational techniques and greater expertise (Kim *et al.* 2016). On the other hand, the equivalent linear method of ground response analysis offers simplicity, ease of implementation, and computational efficiency (Kaklamanos *et al.* 2013; Banerjee *et al.* 2020; Reddy *et al.* 2022), and the same has been portrayed in many studies as well (Choudhury and Savoikar 2009; Pitilakis and Clouteau 2010; Phanikanth *et al.* 2011; Kumar *et al.* 2014; Basu and Dey 2016; Tsiapas and Bouckovalas 2019; Anshu *et al.* 2024; Tallini *et al.* 2024). The equivalent linear approach has even been applied to special treatment as to calibrate the frequency- and pressure-dependent modulus degradation and damping ratio (Yoshida *et al.* 2002; Assimaki and Kausel 2002) as well as in hilly terrains where topographic amplifications are prevalent (Bouckovalas and Papadimitriou 2005).

Based on equivalent linear ground response analysis (ELGRA) approach, this paper elucidates the dynamic response of Itanagar city of Arunachal Pradesh, India. Itanagar, situated in the seismically active Himalayan belt, has experienced the effects of multiple significant earthquakes, including the Shillong (1897, M_w 8.1), Assam (1950, M_w 8.6), and Sikkim (2011, M_w 6.9) earthquakes. These historical events have caused widespread damage across Northeast India, highlighting the critical role of site-specific seismic studies in assessing localized ground amplification effects. Furthermore, the presence of active tectonic structures, such as the Main Frontal Thrust (MFT) and the Main Boundary Thrust (MBT), along with current seismic gap in the Eastern Himalayas, suggests the likelihood of future large-magnitude earthquakes (Bilham 2019). Thus, this study is motivated by the need to evaluate the site response characteristics of Itanagar, employing ELGRA and MASW-derived shear wave velocity (V_s) to develop resilient infrastructure and enhance regional seismic preparedness. Under the umbrella of microzonation studies, although several cities across the Indian territory have been attended with ground response analysis (GRA) studies, yet the North-Eastern state of Arunachal Pradesh had yet remained out of purview, thereby presenting a gap in the literature from this region. Itanagar, the state capital of Arunachal Pradesh, has been declared a smart city (https://www.itanagarsmartcity.org/) and is currently undergoing a hustled infrastructure development over and above the existing ones. In this regard, it becomes imperative to understand the potential vulnerability distribution within the region. Such studies aid in designing earthquake-resistant structures, as well as assessing the seismic health and resilience of existing important structures and improve their life-spans in case they are subjected to forecasted strong motions in the context of an ever-changing tectonic and seismic scenario (Al-Asadi and Alrebeh 2024). MASW was selected over alternative subsurface characterization methods due to its ability to provide spatially continuous shear wave velocity (V_s) profiles with high resolution, making it more effective than sparse borehole-based V_s^{30}assessments (Park *et al.* 1999; Xia *et al.* 2002; Foti *et al.* 2018). Previous works have integrated geophysical techniques such as surface wave analysis and HVSR for seismic site characterization (Khan *et al.* 2021). The MASW technique, when additionally integrated with microtremor analysis, offers a robust and non-invasive approach for seismic site characterization, where MASW-derived shear wave velocity profiles not only correlate well with SPT and borehole data, but also serve as reliable tool in estimating lateral variations in sediment thickness and resonance frequencies across sedimentary basins (Kanli 2010). Additionally, MASW is a non-invasive, cost-effective, and efficient technique, particularly suitable for urban environments in hilly terrain where extensive borehole investigations may not be feasible. Compared to empirical V_s^{30}correlations from Standard Penetration Tests (SPT), MASW offers a higher degree of spatial accuracy in delineating subsurface stratification, thereby ensuring more reliable site response analysis results. In this regard, comprehensive MASW surveys have been undertaken at several places within the urbanized area of the city limits to precisely identify the point-based subsurface profiling and thereby establishing the spatial variation of the subsurface characteristics. The site response is assessed using equivalent linear analysis through the DEEPSOIL, an open-source platform for conducting ground response analysis. This study is aimed to provide a valuable insight into the seismic response of the Itanagar region, highlighting the importance of site-specific geological conditions in influencing ground motion amplification. Therefore, the findings of this analysis can be utilized for the development of more resilient structures and to enhance the seismic risk management strategies in the region.

2. Study Area and Geological Setting

The study area is Itanagar town in Papumpare District, Arunachal Pradesh, India (Fig. 1), with the town centre located at 27°5'12.84" N and 93°36' 31" E. The city is situated within the seismic zone V, having a zone factor of 0.36 and possessing the highest seismic activity as per the Indian seismic code (IS 1893 Part-1 2016). For the present study, Fig. 1 also presents the 22 locations that have been chosen as prominent sites for the MASW survey. The entire Itanagar area is geographically divided into 5 zones. The Northern area (NA) comprises the locations of Botanical Survey of India (BSI), CM House/Mahatma Gandhi Park (CMH/MGP), Indira Gandhi Park (IGP), MOWB-II and Waii International Hotel (WIH). The North-Eastern area (NEA) comprises the locations of Nyokum Ground (NG), Donyi Polo Hotel C-Sector (DPH), Ita Fort (IF) and Government Higher Secondary School (GHSS). The Central area (CA) comprises the locations of Geological Survey of India Chimpu (GSIC), Arunodaya School (AS), RK Mission Hospital (RKMH) and Division-IV (DIV4). The South-Western area (SWA) comprises of the locations Dera Natung Government College (DNGC), Kendriya Vidyalaya 2 (KV2), VIP Housing (VIPH), Sangay Lhaden Sports Academy (SLSA) and State Forest Research Institute (SFRI). The South-Eastern area (SEA) comprises the locations of Chimpu Valley School (CVS), Don Bosco School (DBS), Delhi Public School Itanagar (DPSI) and Jully General Ground (JGG).

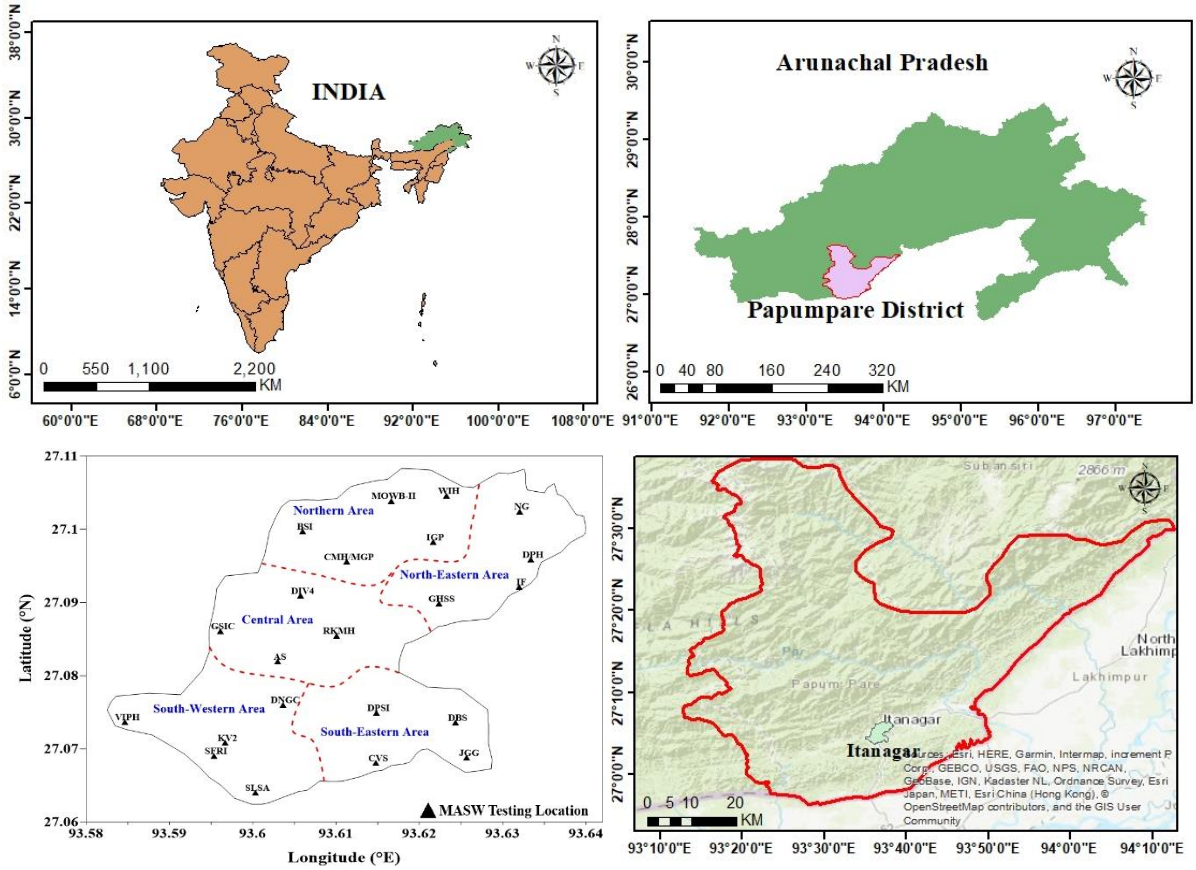

Fig. 1 Geographical position of Itanagar city and the locations of sites for MASW survey

Figure 2 delineates the tectonic components and spatial distribution of the four formations belonging to Siwalik group of rocks in the study area. Debnath *et al.* (2021) have reviewed the lithostratigraphy of the Siwalik Group in the Arunachal Himalaya. There are four classifications of the Siwaliks: Lower Siwalik Dafla Formation, Middle Siwalik Subansiri Formation, Siji Formation (lower part of upper Siwalik) and Upper Siwalik Kimin Formation. The Tipi Thrust places the Dafla Formation above the Kimin/Subansiri Formation in Arunachal Pradesh. Upper Siwalik in Arunachal Pradesh is further divided into two formations - the Siji Formation (mudstone-siltstone-sandstone-conglomerate unit) and the Kimin Formation (conglomerate-sandstone unit) (Debnath *et al.* 2021). Itanagar is well exposed to the middle Siwalik Subansiri Formation, upper Siwalik Siji and Kimin Formations, and south of this is the Lower Siwalik, which is exposed to the north as an upthrust hanging wall block (Mullick and Sinha 2024).

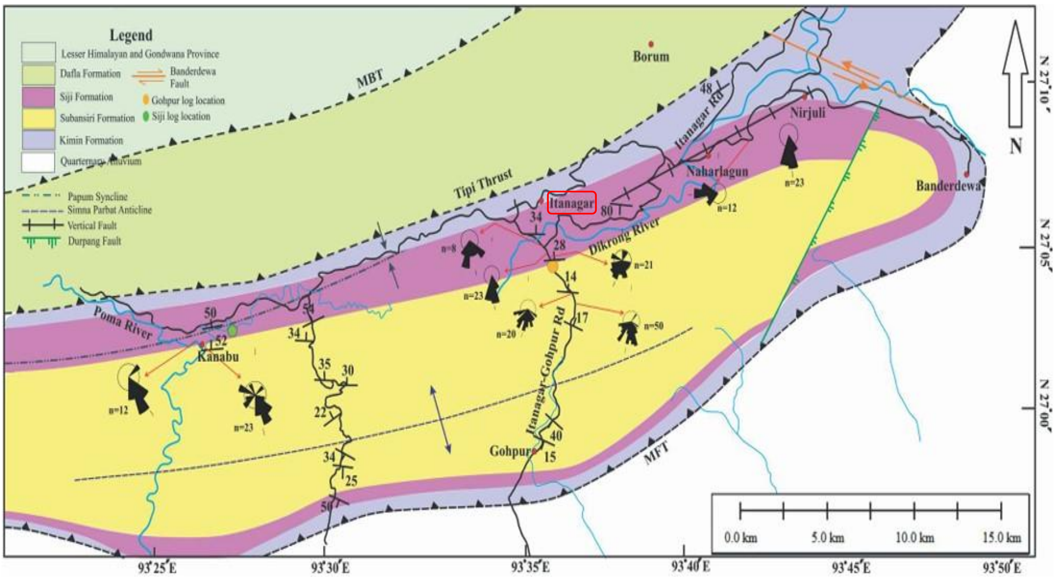

Fig. 2 Tectonic components and spatial distribution of the four Formations belonging to Siwalik group of rocks in and around Itanagar, Arunachal Pradesh, India

3. Methodology

Ground Response Analysis (GRA) includes a range of techniques for evaluating the strong motion-induced response of the soil column and can be achieved in one-, two- or three-dimensional approaches. A one-dimensional equivalent linear GRA, which illustrates the fundamental frequency, amplification factor, and response spectrum of the substrata, is employed in the present study to evaluate the parameters of interest. The equivalent linear method is a simplified approach to model the nonlinear behavior of soil during seismic loading and is implemented in commercial open-source packages such as DEEPSOIL v7.1 (Hashash *et al.* 2024). In this method, the strain-dependent shear modulus and damping of the soil are approximated through an iterative process. The shear wave velocity (V_s) data obtained from MASW surveys serves as a key input that defines the variation of soil stiffness in layered subsurface to be used in the equivalent linear analysis. The accuracy of the MASW data directly impacts the reliability of the computed site response and seismic demands on structures. The MASW technique has been widely used for estimating shear wave velocity profiles and site classification. Studies have shown that integrating MASW with V_{s30} mapping improves site response evaluation and enhances seismic microzonation efforts (Kanli *et al.* 2006; Kanli *et al.* 2008). Integrating high-quality V_s data from MASW into the DEEPSOIL analysis provides a robust framework for seismic site characterization. The stated methodology is applied in the present study to assess the ground response characteristics for Itanagar city.

3.1 Measurement of shear wave velocity using active MASW survey

MASW is a non-destructive seismic exploration technique commended for evaluating subsurface stiffness in 1D, 2D or 3D formats (Park *et al.* 1999). In the active MASW survey, the geophone receivers are arranged in a linear array to capture the seismic waves generated by impulse hammers striking on the ground surface. A seismograph is connected to the receivers through a Data Acquisition System (DAQ). In the present study, a 10 kg sledgehammer is struck on a 30 cm x 30 cm steel plate to generate the seismic signals that travel through the subsurface and are recorded by 24 geophones of 4.5 Hz capacity in form of electrical signals converted from ground vibrations. By analyzing the dispersion and time-history of these signals, MASW analysis identifies the shear wave velocity profile of the subsurface materials (Taipodia *et al.* 2018; Taipodia *et al.* 2018a; Taipodia *et al.* 2021). Figure 3(a) presents a representative schematic diagram of the data acquisition exercise in the field where the geophone array is arranged on the ground surface of the GHSS (i.e. Govt. Higher Secondary School) site at an interval of 1 m and linked through connecting cable that is attached to a Geode seismograph. A near-offset (distance from source to the first receiver) was maintained at 4 m for all the tests after conducting trials with various offset distances. For each of the data acquisition exercise, the sampling time and frequency have been considered as 0.8 s and 4000 Hz, respectively. Five shots are applied one after another consecutively, to generate a stacked shot gather file to avoid the uncertainty/error involved with the actual energy delivered in the test sample (Taipodia *et al.* 2018b). Figure 3b illustrates the time-series collected by the geophone array. As a part of the pre-processing of the collected wavefields, following the recommended proposition (Taipodia and Dey 2017), the noisy region in the time-domain record is muted and filtered out (with the aid of a bandpass filter in a range of 5-180 Hz or likewise as governed by the amplitude spectra of individual site records) as their presence often lead to inaccurate results in the subsurface shear-wave velocity profiles due to the contamination of recorded signals. Figure 3c illustrates a typical dispersion curve generated from the voltage-time records and represented in a phase velocity-frequency domain, along with exhibiting the selected experimental dispersion curve. Further, the extracted dispersion curve is utilized in an iterative inversion process to estimate the shear wave velocity profile at each of the sites. Based on an initially chosen layered earth model as per relevant recommendations (Xia *et al.* 1999; Taipodia *et al.* 2018a), the theoretical dispersion curve is generated and the same is compared to the extracted experimental dispersion curve at the end of each iteration. Based on the disparity between the theoretical and experimental dispersion curve at the end of each iteration, the layered earth model is updated i.e. the parameters defining the earth model such as the Poisson's ratio, density and shear wave velocity of each layer are improvised, while maintaining the thickness of each layer to be unchanged. The process is repeated until the disparity between the experimental and theoretical curve reduces below the tolerance level in the root mean square error (RMSE $\leq$ 10) (Baglari *et al.* 2020). Figure 3d exhibits the experimental dispersion curve (as obtained from Fig. 3c), the initial dispersion curve that is used to commence the inversion analysis and the final dispersion curve obtained at the end of the inversion process. For the GHSS site, the RMS error is found to be 3.26, which is well within the recommended tolerance limit. Finally, Fig. 3e shows the 1-D shear wave velocity profile obtained at GHSS site. Figure 4 exhibits the compiled shear wave velocity (SWV) profiles for all the 22 sites around the Itanagar city study area. The shear wave velocity profile obtained from the MASW survey at each individual location is further used as input parameter to ELGRA studies.

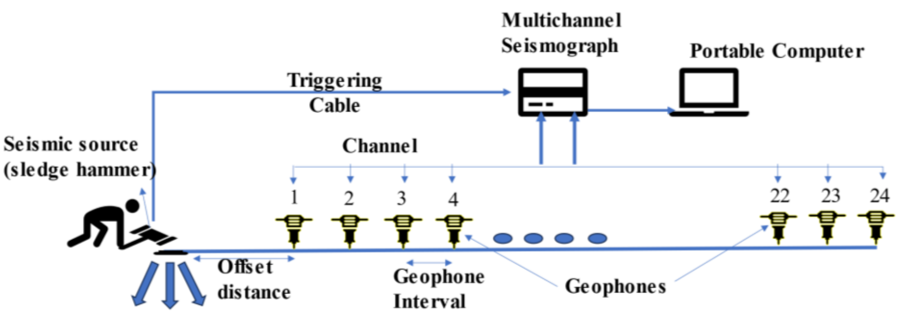

(a)

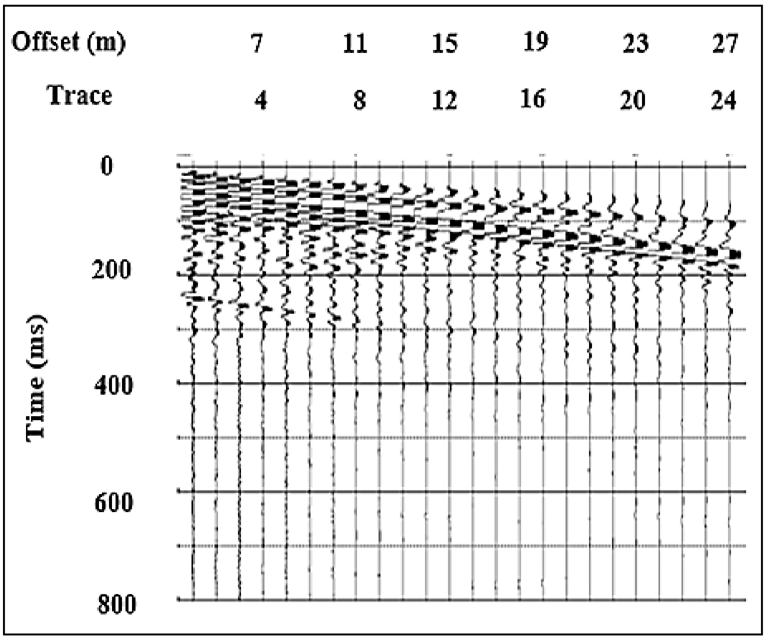
Offset (m)
7
11
15
19
23
27
Trace
4
8
12
16
20
24
Time (ms)
0
200
400
600
800
(b)

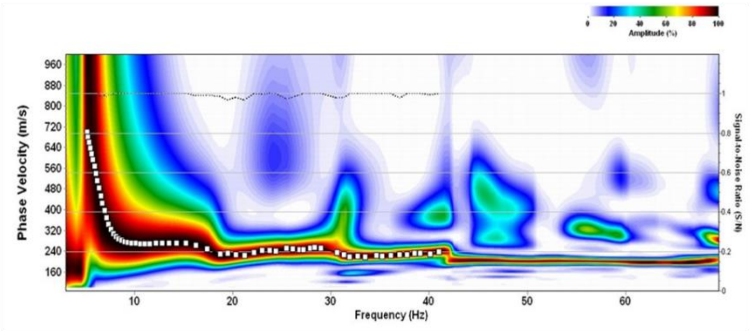
Amplitude (%)
Phase Velocity (m/s)
960
880
800
720
640
560
480
400
320
240
160
10
20
30
40
50
60
Frequency (Hz)
Signal-to-Noise Ratio (S/N)
(c)

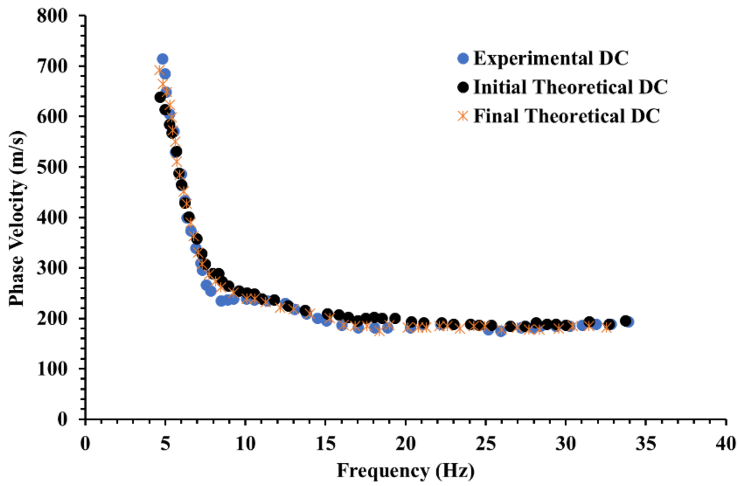
Experimental DC
Initial Theoretical DC
Final Theoretical DC
Phase Velocity (m/s)
800
700
600
500
400
300
200
100
0
0
5
10
15
20
25
30
35
40
Frequency (Hz)
(d)

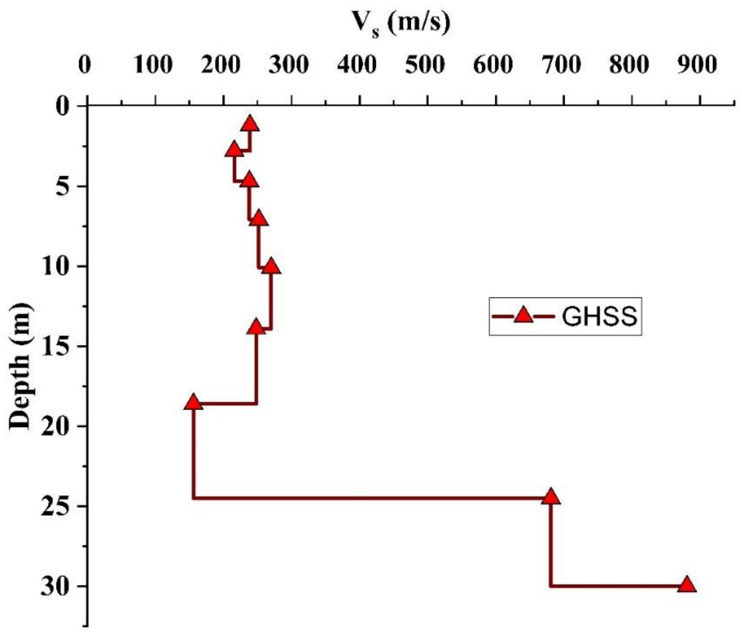

(e)

Fig. 3 A typical representation of MASW analysis conducted for the GHSS site (a) Schematic diagram of field data acquisition (b) Representative seismic waves recorded in geode seismograph (c) Dispersion curve obtained from the MASW record (d) Comparative of the experimental and theoretical dispersion curves during inversion (e) 1-D shear wave velocity profile

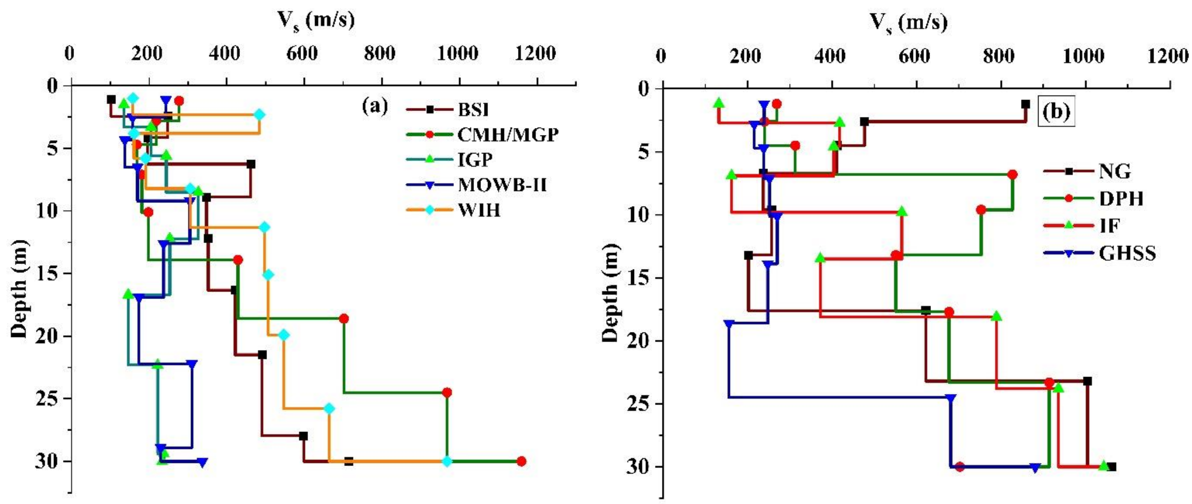

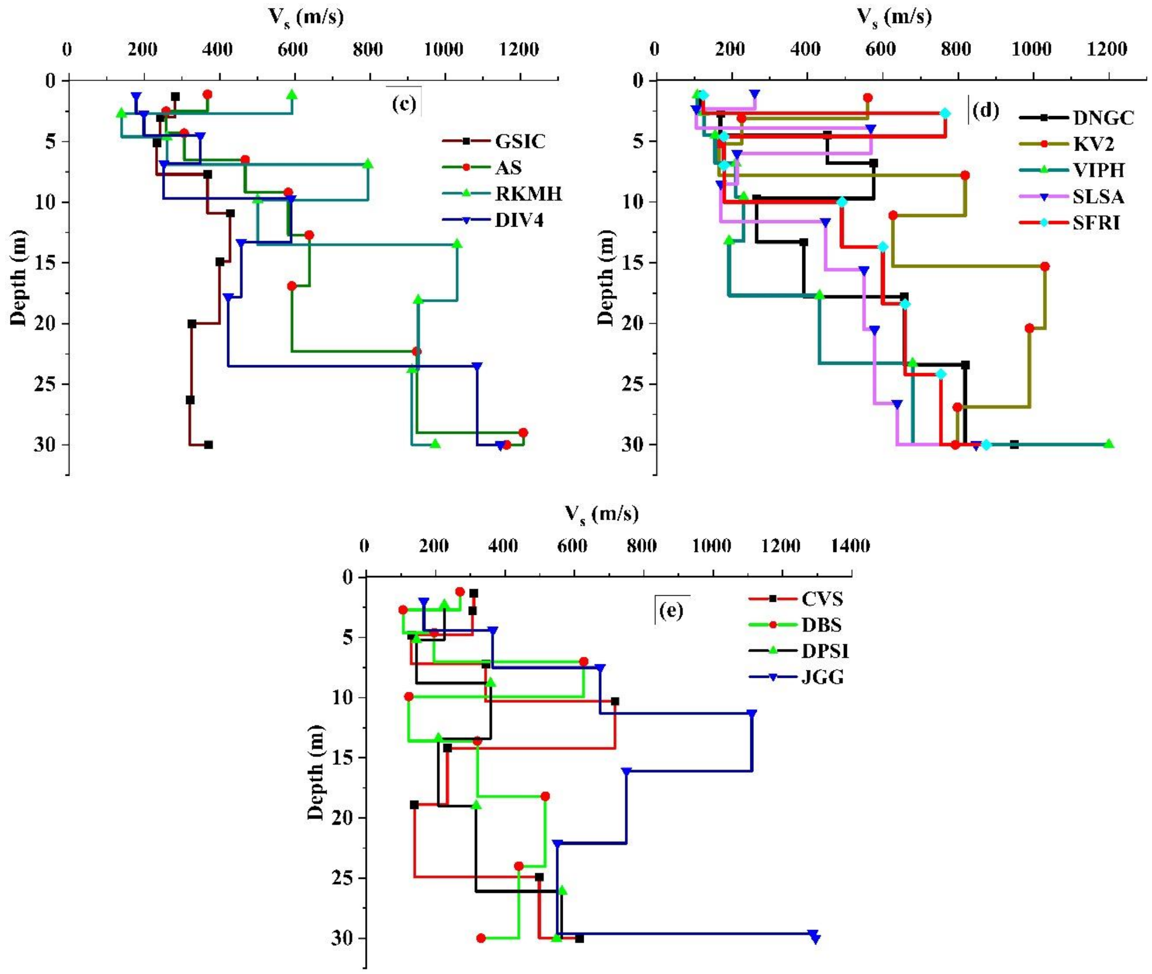

Fig. 4 SWV profile for all test locations (a) Northern area (b) North-eastern area (c) Central area (d) South-west area (e) South- east area of Itanagar city

3.2 Equivalent linear ground response analysis (ELGRA)

The present study uses 1D ELGRA to assess the parameters of ground surface that can be utilized for the design of seismically resilient structures (Kramer 1996; Tempa *et al.* 2021; Kumar and Kumar 2023; Anshu *et al.* 2024). This analysis incorporates Kelvin-Voigt (KV) viscoelastic system with constant shear stiffness and damping factor to account for the soil behavior to assess the response of the medium due to the vertically propagating shear waves. As per the KV model, the shear stress and shear strain relationship is described as

$$\tau = G\gamma + \eta \frac{\partial \gamma}{\partial t} \tag{1}$$

where, τ is the shear stress at any time t, η is the viscous damping coefficient, γ is the shear strain, and G is shear stiffness. The equation of motion for the vertically propagated shear wave, in z-direction, can be described as

$$\rho \frac{\partial^2 u}{\partial t^2} = \frac{\partial \tau}{\partial z} \tag{2}$$

where, ρ is the mass density of the soil medium, and u is the displacement in the horizontal (or, x-direction). Further, combining both the above equations, the equation of motion can be expressed as

$$\rho \frac{\partial^2 u}{\partial t^2} = G \frac{\partial^2 u}{\partial z^2} + \eta \frac{\partial^3 u}{\partial z^2 \partial t} \tag{3}$$

As mentioned earlier, for the present study, DEEPSOIL program has been used to conduct the ELGRA for various sites. For the analysis, the dynamic soil characteristics of sandy soil (i.e. the shear strain-dependent modulus degradation and damping ratio) as proposed by Seed and Idriss (1970) have been opted. Further, in regard to the boundary condition at the bottom of the soil profile, a rigid half-space is chosen to be existent for all locations. In order to establish the compatibility of the nonlinear characteristics of soil compatible to the equivalent linear analysis, the effective shear strain is considered 65% of the maximum shear strain that is assessed in terms of shear strain ratio (SSR) (Kramer 1996). The magnitude of SSR can be estimated from the earthquake magnitude (M) as proposed by Idriss and Sun (1992).

$$SSR = \frac{M-1}{10} \tag{4}$$

3.3 Strong motions and corresponding acceleration-time history

The acceleration-time history, which represents the distribution of seismic energy over time, is a crucial input parameter for performing seismic GRA. Consequently, four different earthquake motions with varying peak bedrock acceleration (PBAs) are selected as input acceleration-time histories such that the wide spectrum of ground response of the study region can be delineated. The PBAs of the chosen Tezpur EQ (2012, M_w5), Sikkim EQ (2011, M_w6.9), Indo-Burma EQ (1988, M_w7.3) and Kobe EQ (1995, M_w6.9) strong motions are 0.026g (very low-intensity), 0.15g (low-intensity), 0.343g (moderate-intensity) and 0.82g (high-intensity), respectively, thereby considering wide spectrum of seismic intensity of earthquakes in the ground response analysis. Since three of these earthquakes (Tezpur, Sikkim, and Indo-Burma) originate from the seismic sources influencing Itanagar, they appreciably represent the seismic hazards affecting the region. Including a high-energy event (Kobe 1995) allows conducting the ground response analysis under severe earthquake conditions that could potentially impact the Itanagar region in the future. This study utilizes recorded earthquake motions for seismic GRA to ensure regional relevance and capture a wide range of seismic intensities. Figure 5 illustrates the acceleration-time histories of the four input motions. Additionally, using Seismosoft (2012), various strong motion characteristics (Kramer 1996) such as Arias intensity, V_{max}/A_{max}, a frequency content parameter represented by the ratio of maximum ground velocity (V_{max}) to the maximum ground acceleration (A_{max}) during a seismic event], predominant period, mean period, bracketed duration, and significant duration, were calculated and are summarized in Table 1. Figure 6 clearly exhibits that the chosen strong motions significantly differs in their energy characteristics in both the time- and frequency-domain, thereby indicating that variations in the chosen strong would sufficiently reflect the variations in the ground response analyses that would be described in the subsequent sections.

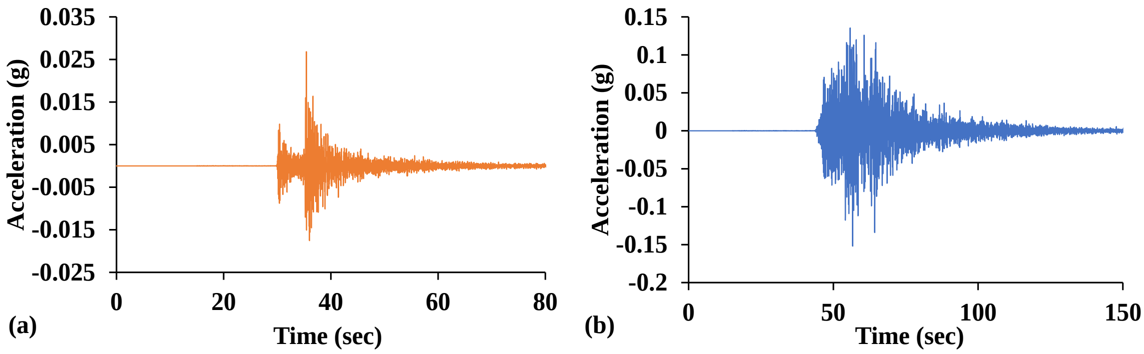

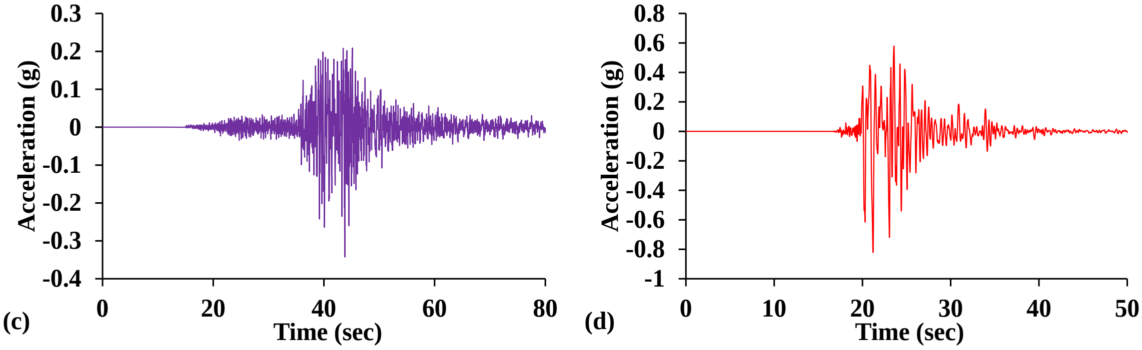

Fig. 5 Acceleration-time history of various strong motions (a) 2012 Tezpur (b) 2011 Sikkim (c) 1988 Indo-Burma (d) 1995 Kobe

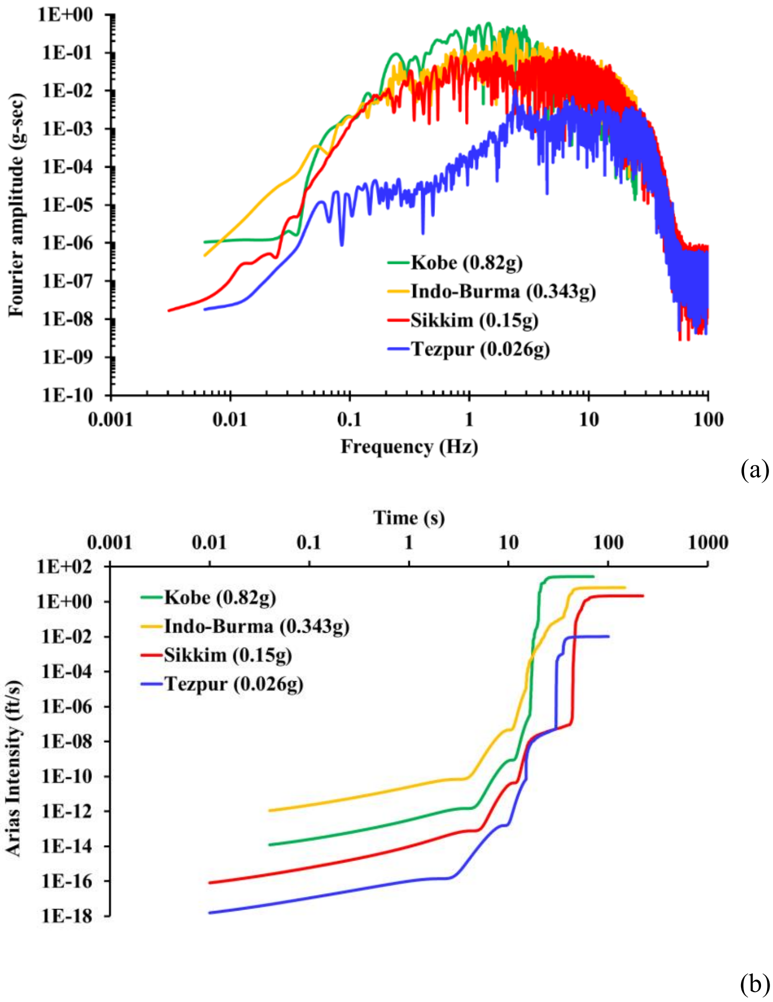

Fig. 6 Comparative (a) Fourier amplitude spectra and (b) Arias intensity of the chosen strong motions

Table 1 Strong motion characteristics for various earthquakes chosen for present study

Strong motion parameters	**Tezpur (2012)**	**Sikkim (2011)**	**Indo–Burma (1988)**	**Kobe (1995)**
Date	19-08-2012	18-09-2011	06-08-1988	17-01-1995
Magnitude (M_w)	5	6.9	7.3	6.9

PGA (g)	0.026	0.15	0.343	0.82
Predominant period (s)	0.22	0.14	0.44	0.36
Mean period (s)	0.211	0.27	0.413	0.648
Bracketed duration (s)	39.25	71.72	78.49	21.45
Significant duration (s)	10.01	31.75	19.55	8.34
Arias intensity (m/s)	0.984	0.665	1.88	8.29
Specific energy density (cm^2/s)	95.10	185.93	760.98	7541.71
Cumulative absolute velocity (cm/s)	898.79	1164.42	1747.17	2076.23
V_{max}/A_{max} (s)	0.0326	0.074	0.065	0.101

4. Results and Discussions

Based on the stated input considerations, the findings from ELGRA are represented in terms of acceleration profiles, amplification/deamplification of seismic waves, displacement profile, shear strain profile, and shear stress variation with depth, as well as spectral acceleration (SA) at the surface level for the Itanagar region.

4.1 *Spatial variability of ground acceleration and amplification factors*

This section presents the variation of peak horizontal acceleration along with the amplification or deamplification profiles of seismic wave for the chosen strong motions. Figures 7(a-e) illustrate the outcomes from the ELGRA, thereby showcasing the impact of site-specific substrata on the response characteristics of various locations selected for this study. Figure 7a depicts the variations in peak horizontal acceleration with depth across different test sites, thereby revealing that each soil site responds distinctively during earthquakes that is influenced by substrata variations. The free-field PGA at the surface was found to range 0.064g-0.290g (the bounding profiles are exhibited by the black dotted lines) when subjected to PBA = 0.026g (Tezpur motion), thereby indicating an amplification of seismic wave at all sites. The amplification factor (ratio of the peak acceleration at the ground surface to the peak acceleration at the bedrock) of seismic waves at the surface level ranged 1.5-11, as shown in Fig. 7b. For both the Figs. 7a and 7b, the solid coloured lines indicate the approximate average of the acceleration profile and amplification factor obtained in each zone of Itanagar city (as demarcated in Fig. 1c). It can be noted that the average surface amplification factor in each of the zones range within 4-7 times with respect to the input Tezpur motion with PBA = 0.026g.

Figure 7c presents the variation of displacement with depth for different places when subjected to Tezpur input motion (0.026g). On an average, the zonal displacement profiles are not substantially different from each other. However, it is noted that sites with higher displacement in the upper layers mostly have softer or looser soils, making them more susceptible to ground motion. GHSS and Chimpu valley school exhibit higher displacements throughout the depth profile compared to others. Gazetas (1991) indicates that homogeneous soils show more uniform displacement with depth, while layered soils exhibit more complex patterns. Figure 7d portrays the variation of percentage strain with depth at different places when subjected to Tezpur strong motion (0.026g). There is significant variation in strain among different locations. On an average, it can be noticed that entire Itanagar city exhibits a relatively higher percentage of strain in the shallower depths (3-10 m), suggesting more flexible or less compacted materials and that these areas are more responsive to surface motion, which is critical for infrastructures with shallow foundations. Furthermore, both the North-eastern and South-eastern parts of Itanagar city shows higher strains at deeper depths of 12-18 m as well, thereby signifying its importance for deeper level pile foundations as well.

Figure 7e depicts the variation of the shear stress ratio with depth for different places when subjected to input motion from Tezpur (0.026g). The shear stress ratio is described as the ratio of shear stress generated to the effective overburden pressure. The shear stress ratio decreases with depth that is attributed to the fact that the deeper soils are more consolidated and have higher shear strength. Softer soils tend to have higher shear stress ratios, especially, near the surface (Kaklamanos *et al.* 2011). It can be observed that on an average, the Central and North-Eastern area of Itanagar city shows higher shear stress ratios than the other regions. Additionally, contour maps of maximum acceleration (A_{max}) and amplification factor at the surface level are shown in Fig. 8a and Fig. 8b, respectively. It is observed that parts of North-Eastern (IF), South-Eastern (JGG), Central (RKMH, AS) as well as South-Western (DNGC, KV2) areas exhibit significant amplification. These maps will be valuable for structural design in the Itanagar region, particularly when considering ground motion with a PBA of 0.026g.

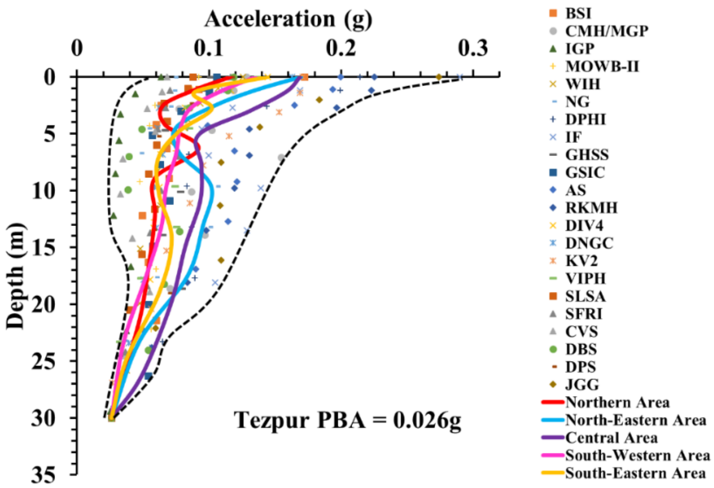

(a)

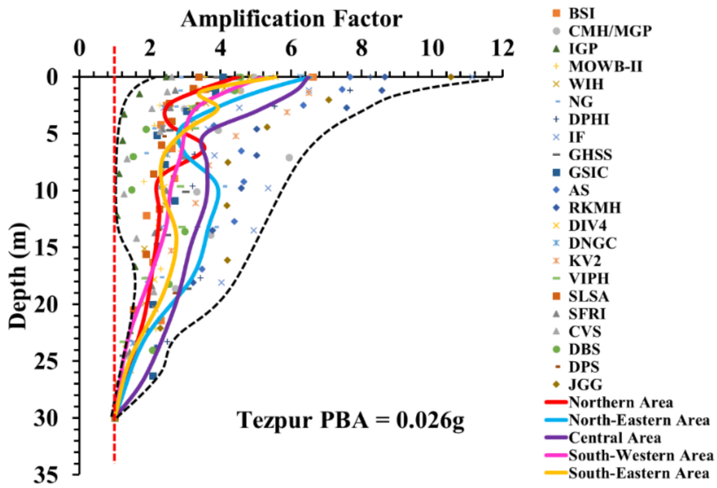

(b)

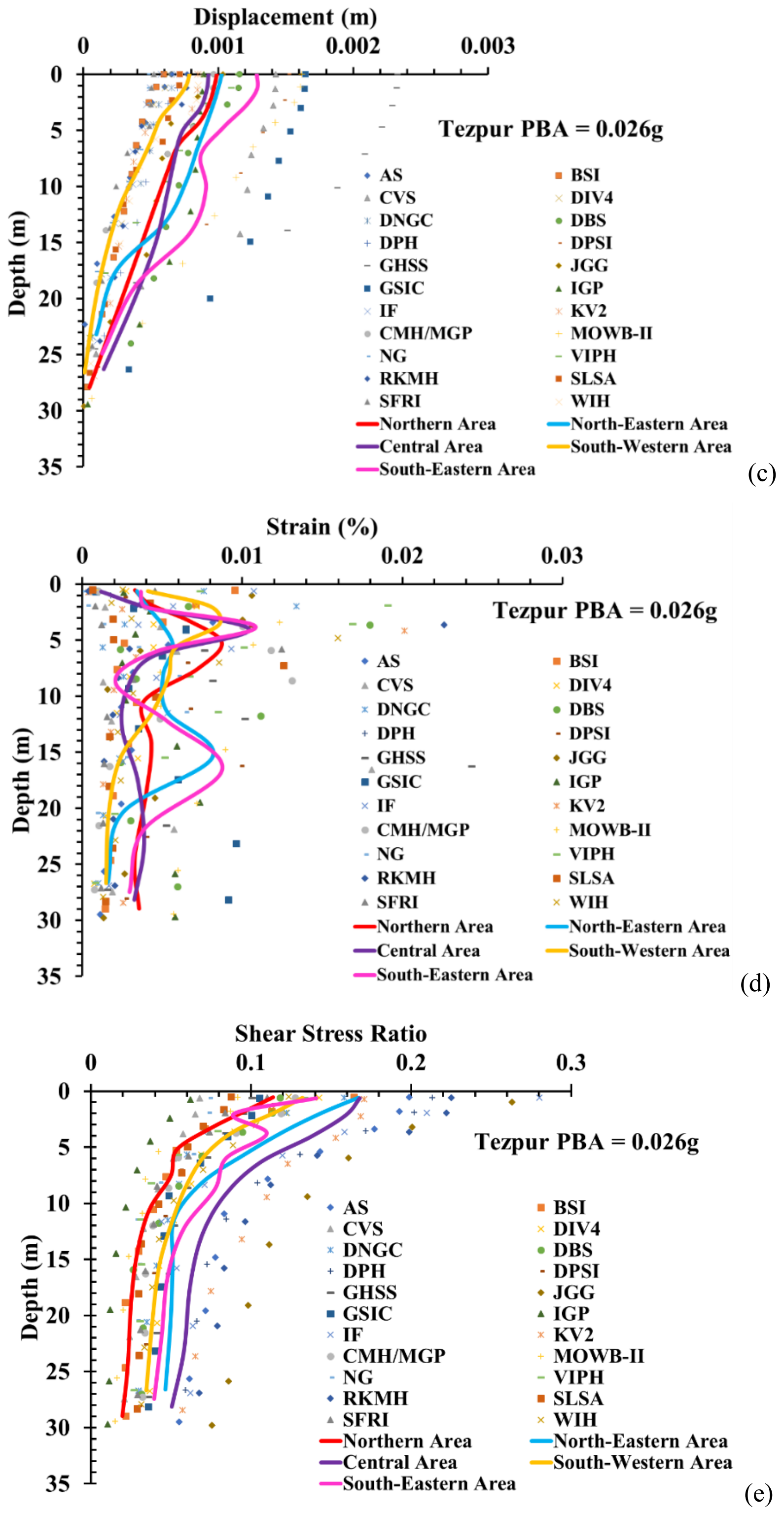

Fig. 7 Variation of (a) peak ground acceleration, (b) seismic wave amplification, (c) displacement, (d) shear strain and (e) shear stress ratio along with depth using 2012 Tezpur strong motion (PBA = 0.026g)

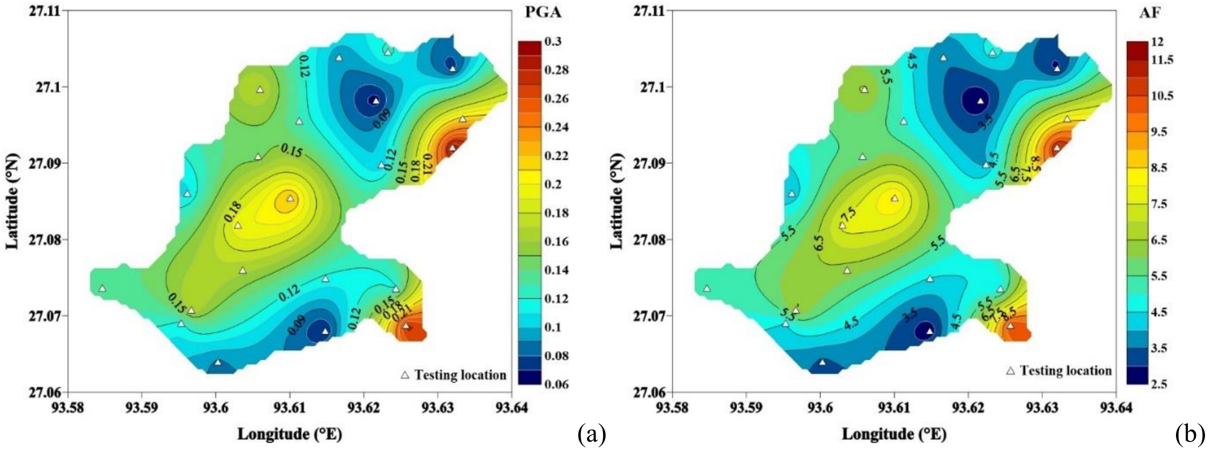

Fig. 8 Contour map of (a) surface PGA and (b) amplification factor in Itanagar region developed from 2012 Tezpur strong motion (PBA = 0.026g)

Further analyses are conducted using the different strong motions chosen for the present study. Figures 9, 10 and 11 exhibit the contour maps of surface PGA and amplification factors for the study area when subjected to Sikkim strong motion (PBA = 0.15g), Indo-Burma strong motion (PBA = 0.343g) and Kobe strong motion (PBA = 0.82g), respectively. With the gradual increase in the PBA of the strong motions, it could be noticed that the surface PGA and amplification factor of the entire region keeps on increasing and the earlier mentioned site locations (IF, JGG, RKMH, AS, DNGC and KV2) attains a more vulnerable state. When subjected to Sikkim, Indo-Burma and Kobe motions, the surface PGA is found to be in the range of 0.236g-1.127g, 0.247g-1.327g and 0.326-1.709g, respectively, while the amplification factors are found to vary in the range of 1.57-7.51, 0.72-3.87 and 0.4-2.1, respectively. It is interestingly noted that the although the PGA increases with the increase in the PBA of the strong motions, the amplification factors decrease. This is attributed to the well-established fact that higher PBA of a strong motion would induce more strains and displacements in the soil column subjected to ELGRA (Basu *et al.* 2017; Kumar *et al.* 2018; Dey *et al.* 2021; Anshu *et al.* 2024). Figure 12 exhibits the increment in the average displacement and strain profiles of various zones of Itanagar city (as shown in Fig. 1) when subjected to various strong motions of increasing PBA. The induced shear strain remains within the elastic or near-elastic range ($\gamma \leq 0.01\%$), where damping effects are minimal and thereby, amplification remains high (Basu *et al.* 2017; Basu *et al.* 2019). As PBA increases to moderate levels (e.g. 0.15g Sikkim motion), the shear strain reaches nonlinear threshold ($\gamma \approx 0.05\%$–0.1%), leading to a reduction in shear modulus and an increase in damping, which limits further amplification. At higher PBA levels (e.g. 0.343g Indo-Burma and 0.82g, Kobe motions), significant shear strain occurs ($\gamma \geq 0.2\%$), resulting in increased damping values which dissipates seismic energy and thereby reducing the amplification factor. As the damping increases with the strain (Seed and Idriss 1970), the amplification of the bedrock motion decreases as the seismic wave reaches the ground surface. For few specific sites (namely IGP, CVS, GHSS, GSIC, MOWB-II, DPS, CMH/MGP, SLSA), as reflected in Fig. 13, deamplifications up to larger depths can be noticed with the increase in the PBA of the strong motions. The observed reduction in amplification at higher PBAs can also be generically attributed to the combined influence of lithological transitions, depth-dependent damping variations, and local topographical effects. The presence of heterogeneous soil layers and buried bedrock interfaces can further contribute to impedance contrasts, influencing wave propagation and causing localized deamplification. The spatial variation in amplification factors across different locations (Figures 8–11) is influenced by subsurface soil characteristics. Sites such as IGP, CVS, GHSS, and GSIC exhibit deamplification due to substantial softer soil deposits, which limit wave propagation effects. Conversely, sites such as JGG, IF, RKMH, AS, DNGC, and KV2 show higher amplification, likely due to the presence of moderately softer alluvial deposits, which enhance seismic wave amplification. Variations in sedimentary layering and depth-dependent changes in shear wave velocity significantly contribute to differential site response, thereby influencing seismic wave propagation and amplification effects. Figure 14 exhibits the variation of shear stress ratio profiles averaged for various zones of Itanagar city. The shear stress ratio exhibits significant variability across different sites, reflecting the influence of surface soil properties and local conditions. As the depth increases, the shear stress ratio tends to sufficiently decrease, thereby indicating the transition to more consolidated geological layers that exhibit lower stress ratios (Stewart *et al.* 2002; Rathje *et al.* 2015; Wang *et al.* 2017). It can also be noted from Fig. 14 that under high PBA strong motion (such as 0.82g Kobe motion), Central area of Itanagar city shows exceedance of SSR=1 up to significant depth, thereby indicating the possible vulnerability of the demarcated area. High magnitudes of SSR might trigger loss of bearing and enhanced soil-structure interaction scenarios, and demands additional attention when the typology of infrastructures are to be decided for the area. Except under this specific scenario, Itanagar city can be adjudged fairly safe against significantly detrimental seismic hazard in regard to the earthquake-induced stresses beneath infrastructures.

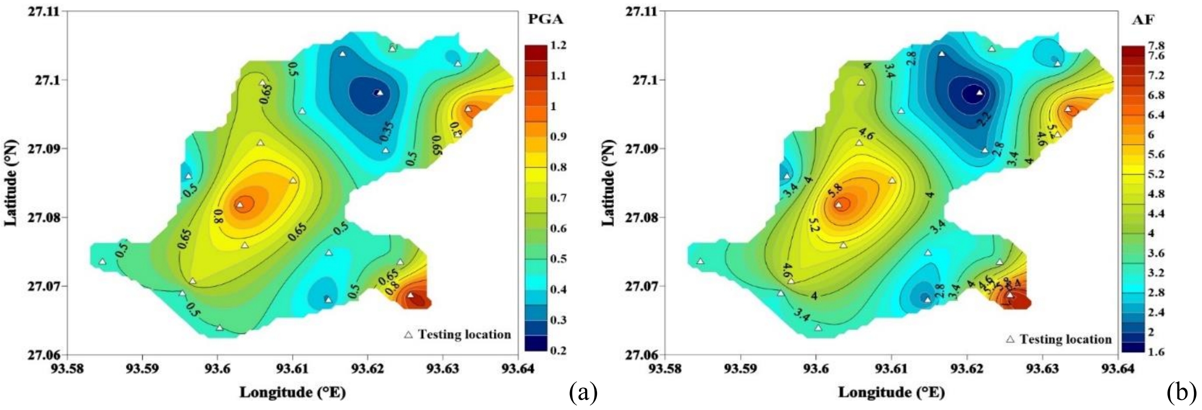

Fig. 9 Contour map of (a) surface PGA and (b) amplification factor in Itanagar region developed from 2011 Sikkim motion (PBA = 0.15g)

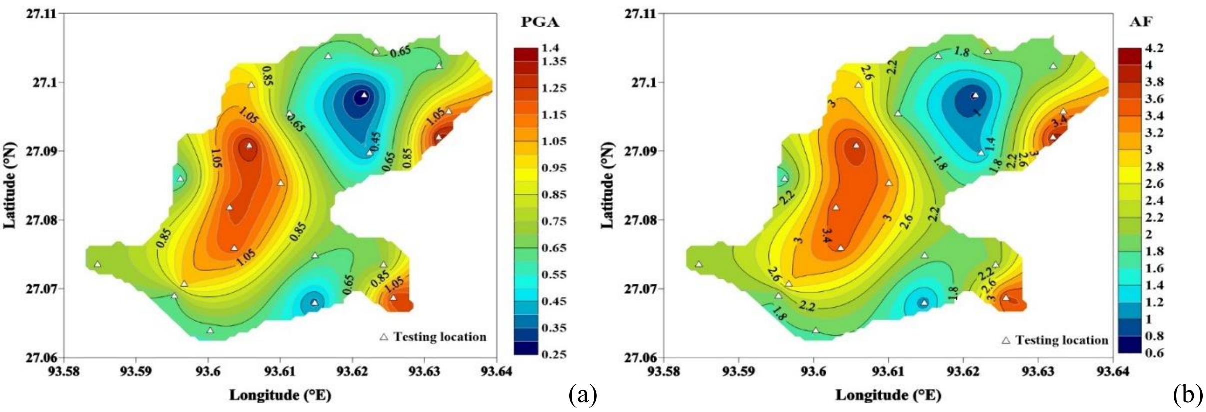

Fig. 10 Contour map of (a) surface PGA and (b) amplification factor in Itanagar region developed from 1988 Indo-Burma motion (PBA = 0.343g)

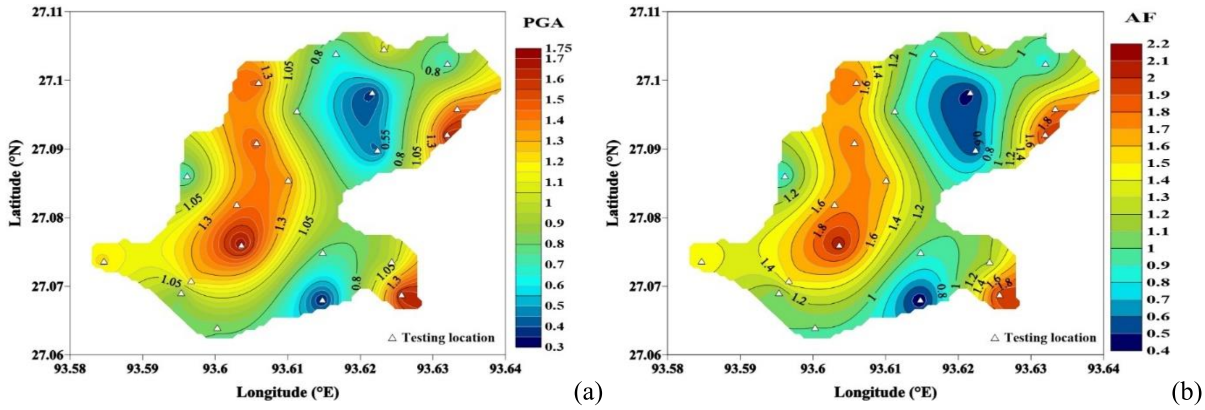

Fig. 11 Contour map of (a) surface PGA and (b) amplification factor in Itanagar region developed from 1995 Kobe motion (0.82g)

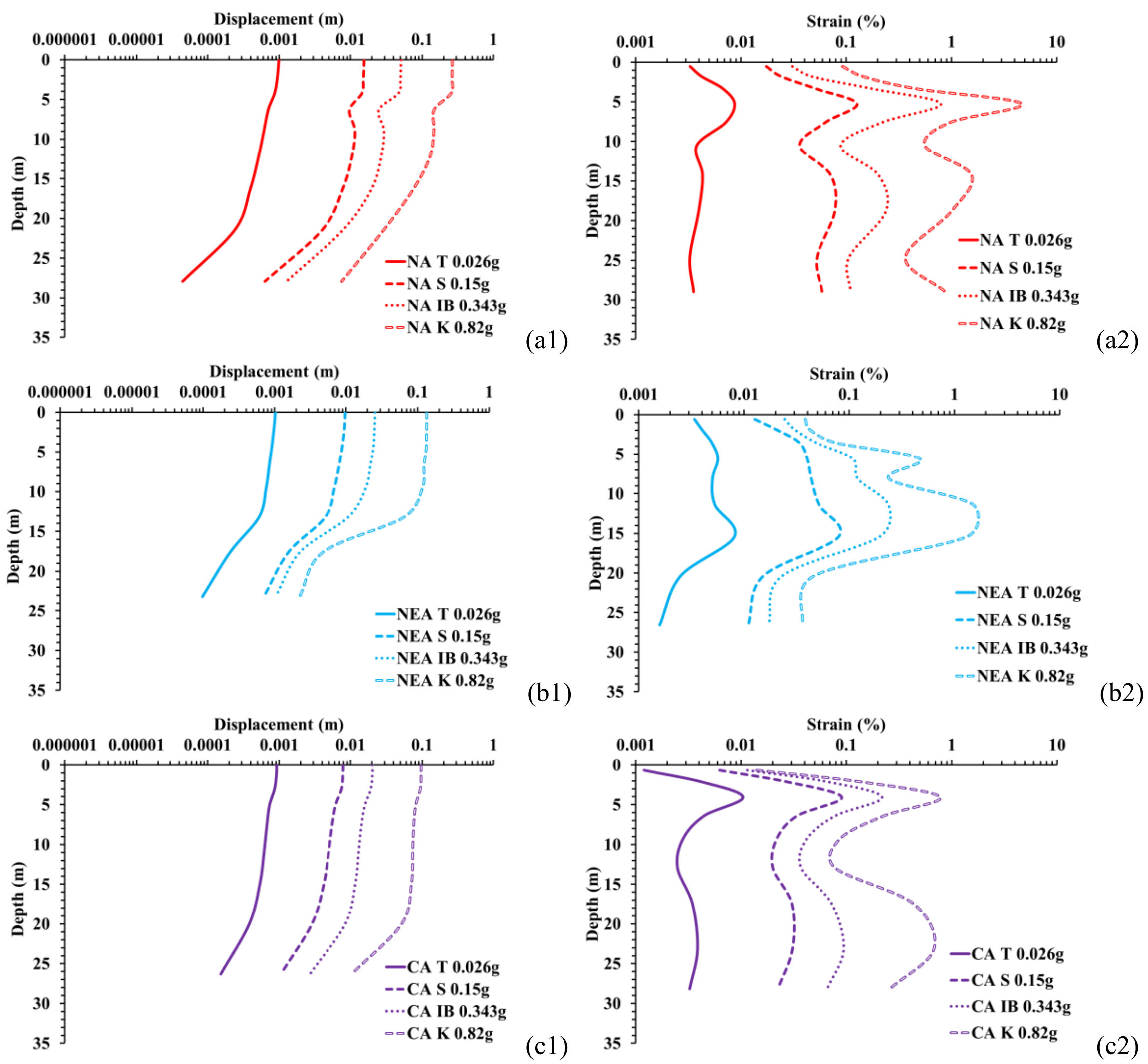

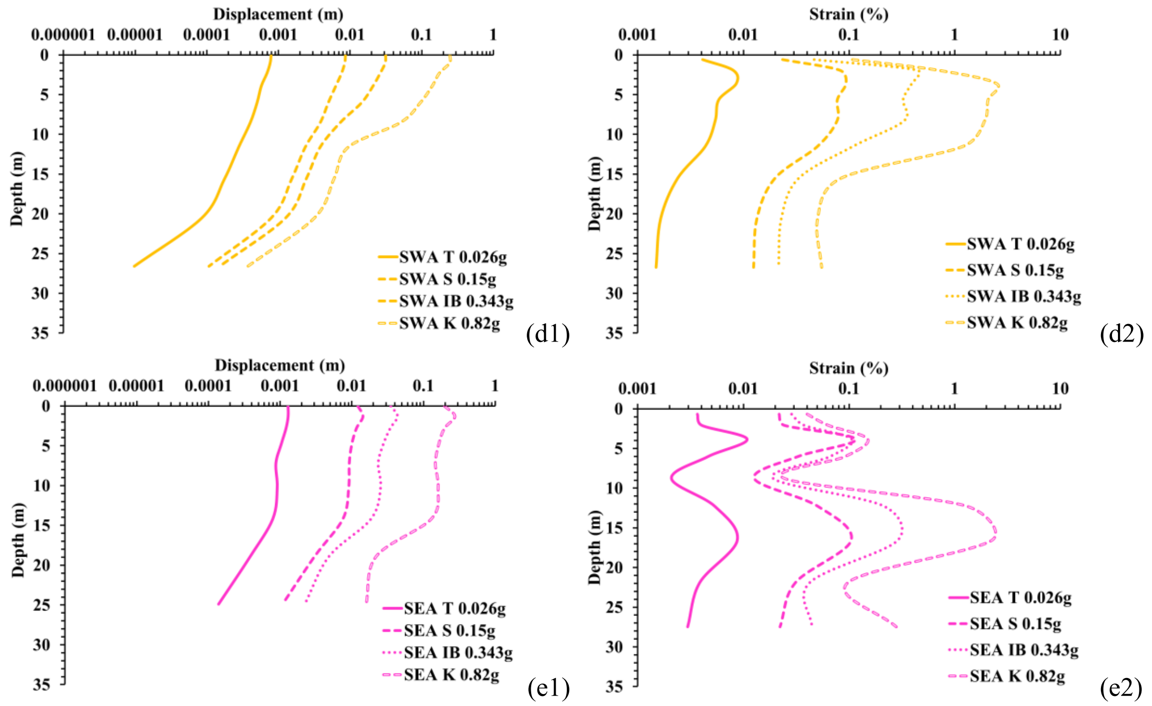

Fig. 12 Influence of PBA on the average (a1-e1) displacement profiles and (a2-e2) percentage strain profiles of the various zones in Itanagar city

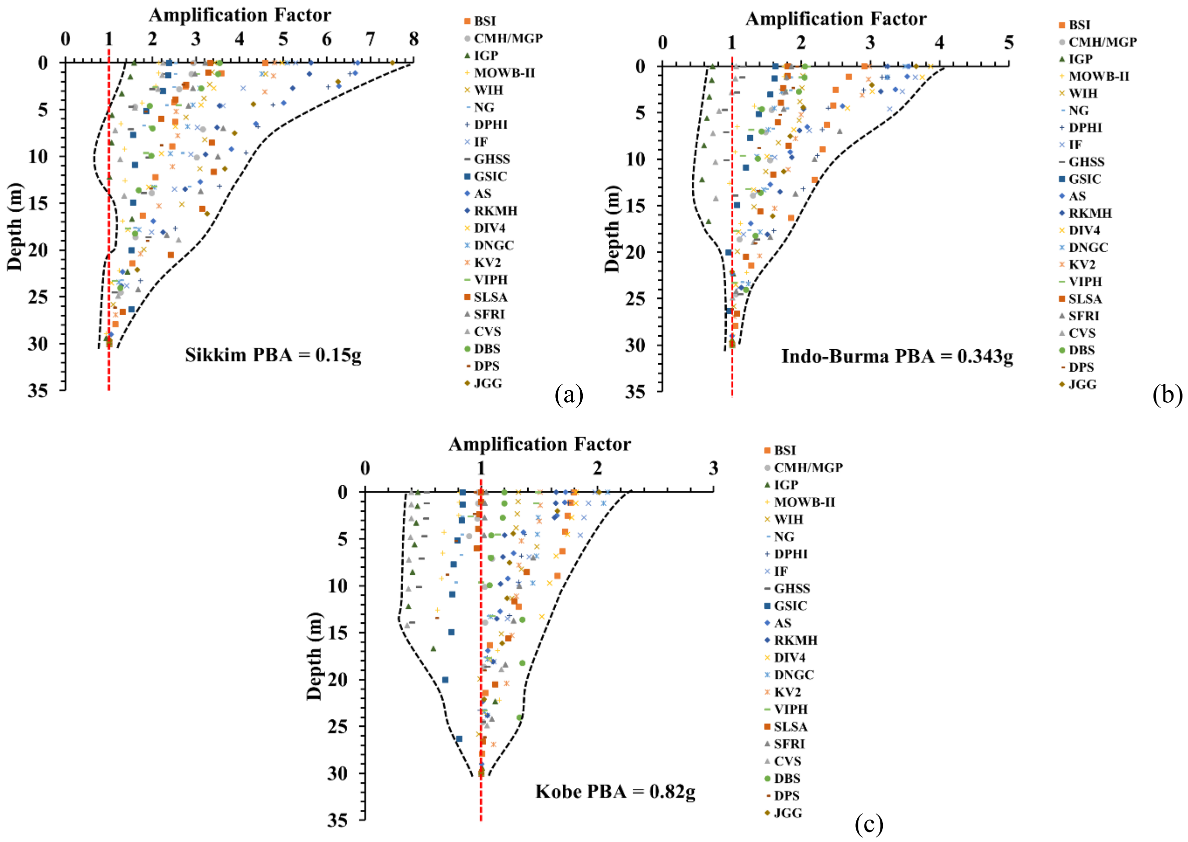

Fig. 13 Profiles of amplification factor for all sites developed from (a) 0.15g Sikkim motion (b) 0.343g Indo-Burma motion and (c) 0.82g Kobe motion

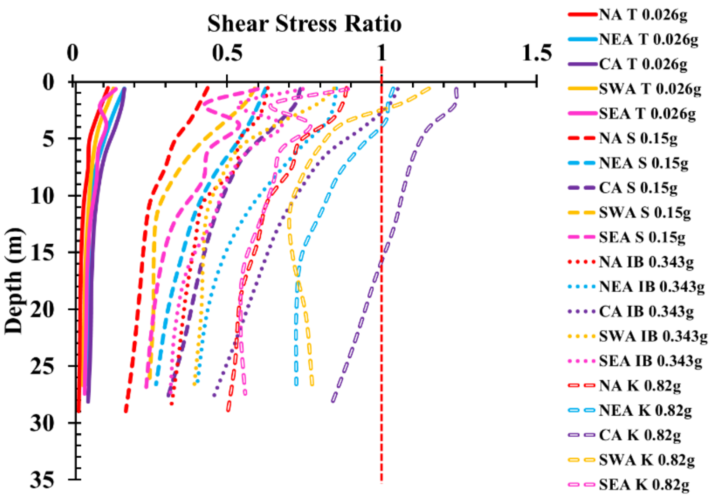

Fig. 14 Profiles of shear stress ratio averaged at various zones of Itanagar city when subjected to different strong motions

Table 2 illustrates the surface level acceleration and amplification factors, showing that the A_{max} and amplification factors for all 22 sites are higher when using the Kobe earthquake motion (PBA=0.82g) compared to other input motions. This can be attributed to the influence of ground motion parameters, such as the significant duration listed in Table 1. Consequently, it is essential to study the impact of other strong motion characteristics, such as duration and frequency content parameters, on GRA, in addition to variations in amplitude parameters like PBA.

Table 2 Summary of the results of acceleration at the surface level and the amplification factor

Location Name	Acceleration (g) at Surface Level				Amplification Factor (AF)			
	Tezpur (2012)	Sikkim (2011)	Indo-Burma (1988)	Kobe (1995)	Tezpur (2012)	Sikkim (2011)	Indo-Burma (1988)	Kobe (1995)
AS	0.20	1.01	1.22	1.41	7.67	6.71	3.55	1.73
BSI	0.17	0.69	1.00	1.47	6.62	4.58	2.91	1.79
CVS	0.07	0.34	0.36	0.33	2.62	2.24	1.06	0.40
DIV4	0.14	0.75	1.33	1.49	5.56	4.98	3.87	1.82
DNGC	0.16	0.77	1.20	1.71	6.26	5.10	3.50	2.09
DBS	0.12	0.53	0.70	0.98	4.56	3.53	2.05	1.20
DPH	0.21	0.99	1.10	1.45	8.24	6.63	3.21	1.77
DPSI	0.12	0.43	0.66	0.77	4.48	2.88	1.92	0.94
GHSS	0.10	0.35	0.40	0.43	3.90	2.35	1.16	0.53
JGG	0.27	1.13	1.26	1.65	10.53	7.51	3.66	2.01
GSIC	0.11	0.36	0.56	0.69	4.07	2.38	1.62	0.84
IGP	0.06	0.24	0.25	0.37	2.45	1.57	0.72	0.45
IF	0.29	0.79	1.33	1.62	11.14	5.29	3.87	1.98
KV2	0.17	0.72	1.02	0.24	6.57	4.80	2.99	1.51
CMH/MGP	0.13	0.44	0.62	0.80	4.94	2.94	1.80	0.97
MOWB-II	0.09	0.32	0.60	0.67	3.55	2.15	1.76	0.81
NG	0.07	0.38	0.63	0.68	2.84	2.50	1.84	0.83
VIPH	0.14	0.49	0.72	1.22	5.25	3.28	2.09	1.49
RKMH	0.23	0.85	1.11	1.35	8.66	5.64	3.25	1.64
SLSA	0.09	0.50	0.62	0.82	3.38	3.32	1.81	1.00
SFRI	0.12	0.48	0.64	0.85	4.48	3.21	1.86	1.04
WIH	0.13	0.51	0.70	1.08	4.83	3.43	2.03	1.32

4.2 *Influence of local site effects on spectral acceleration*

In ground response analysis studies, the maximum Spectral Acceleration (SA_{max}) represents the peak response of structural mass under free-field conditions, which is crucial for developing design spectral acceleration. The free-field design response spectrum can be used to design seismically resilient structures as it incorporates the effects of site geology and soil properties. The design spectral acceleration is represented by an average smoothened graph that illustrates maximum acceleration (A_{max}) for the expected earthquake at the base of a single degree of freedom system, based on its natural frequency or period of oscillation (Kramer 1996). This plot enables engineers to select a design acceleration value considering the PBA, soil conditions, and time period. Additionally, this graph aids in adjusting the spectral acceleration and structural design to enhance building safety during earthquakes, especially if anticipated earthquake accelerations exceed the design value. For all sites, Fig. 15a presents the maximum spectral acceleration at the surface level for all sites using input ground motions of Indo-Burma (0.343g) strong motion. It can be noted that among all the MASW testing locations, the SA_{max} at the DIV4 site is maximum (i.e., SA_{max} = 8.05g) and it occurs at a period of 0.253s. In comparison to the spectral accelerations of soft, medium and hard soil as recommended in IS 1893 Part-1 (2016), significantly high spectral acceleration is obtained at many of the sites namely JGG, DPH, AS, IF, DNGC, KV2, BSI and RKMH. The majority of the peaks occur within the period of approximately 0.2-0.4s, indicating that most sites experience the highest acceleration at short periods, which is typically associated with soft to medium stiff surface soils capable of amplifying high-frequency ground motion. Additionally, variations in sediment stratification and impedance contrast at different depths influence seismic wave propagation, further amplifying spectral acceleration at these locations. Figure 15b presents the 5% damped spectral acceleration at all sites when subjected to the Tezpur motion (0.026g). It can be observed that although the spectral accelerations remain relatively more for the above-stated site locations, yet the damped spectral acceleration magnitudes are significantly lower than that obtained with the Indo-Burma motion. Further, it is also noted that the spectral peaks occur at comparatively lower periods (0.05-0.2s) when subjected to the Tezpur motion. Thus, based on the above comparisons, it can be stated that the site responses are more severe when subjected to higher PGA motions and the existing or proposed infrastructures would be more vulnerable when subjected to Indo-Burma motion or others with higher PBA. These are critical observations for engineering and design purposes, as structures with natural periods in these range may experience significant seismic forces when subjected to higher PBA motions. Figure 16 presents the contour map of SA_{max} at surface level at all 22 sites to highlight the influence of soil variability on spectral accelerations and clearly demarcating the areas of Itanagar city that should need special attention in terms of seismic response analysis of ongoing or upcoming infrastructure development. The contour maps illustrate higher SA_{max} values in Central, South-Western and some parts of North-Eastern areas, thereby highlighting significant seismic amplification in regions with relatively softer soils in the upper layers, while lower spectral acceleration values at the peripheral regions signifying presence of stiffer soils. Figure 17 exhibits the comparative spectral accelerations averaged over the regions, thereby exhibiting the vulnerability of the above stated zones of Itanagar city to earthquakes with higher PBA within the periods of 0.2-0.4 s.

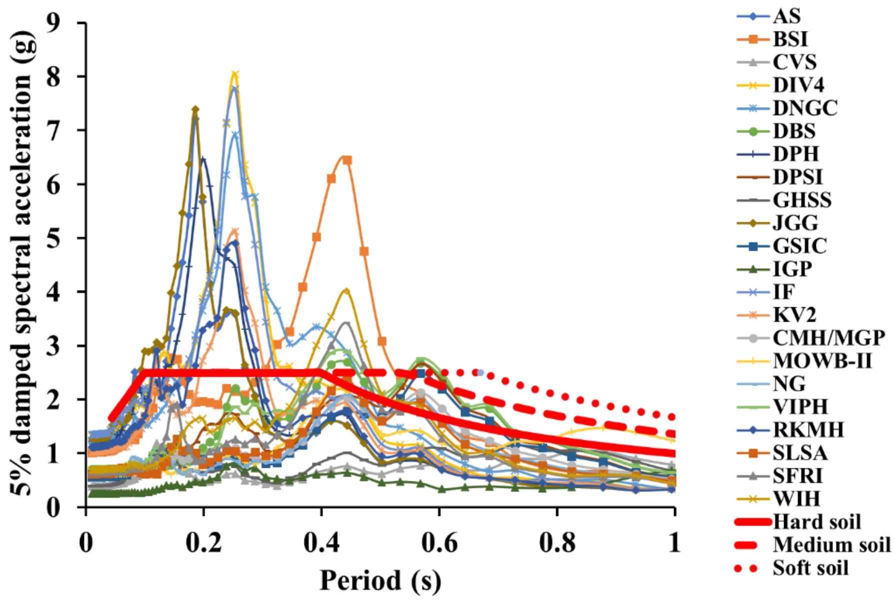

(a)

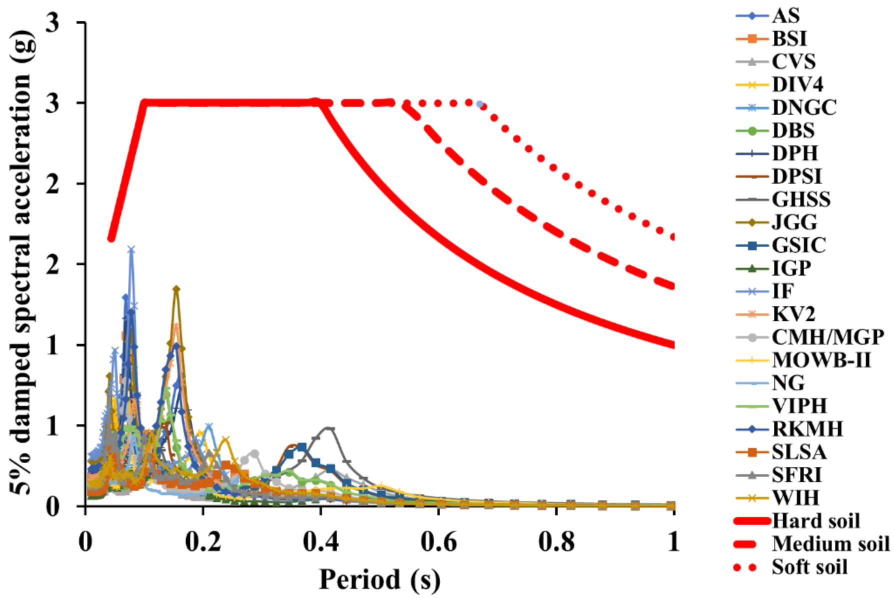

(b)

Fig. 15 5% damped spectral accelerations at the surface of all MASW testing locations using (a) Indo-Burma motion (b) Tezpur motion

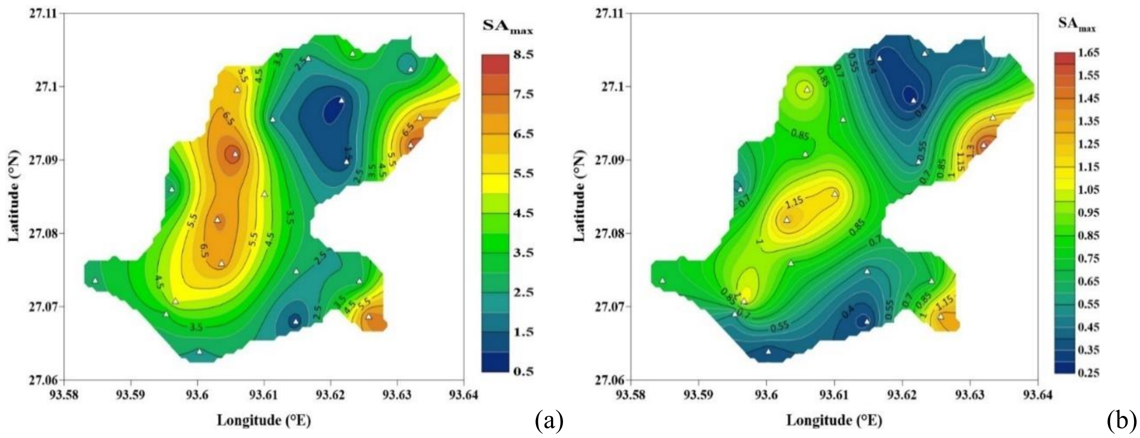

Fig. 16 Contour map of maximum spectral acceleration at surface level in Itanagar region developed using (a) 0.343g Indo-Burma motion (b) 0.025g Tezpur motion

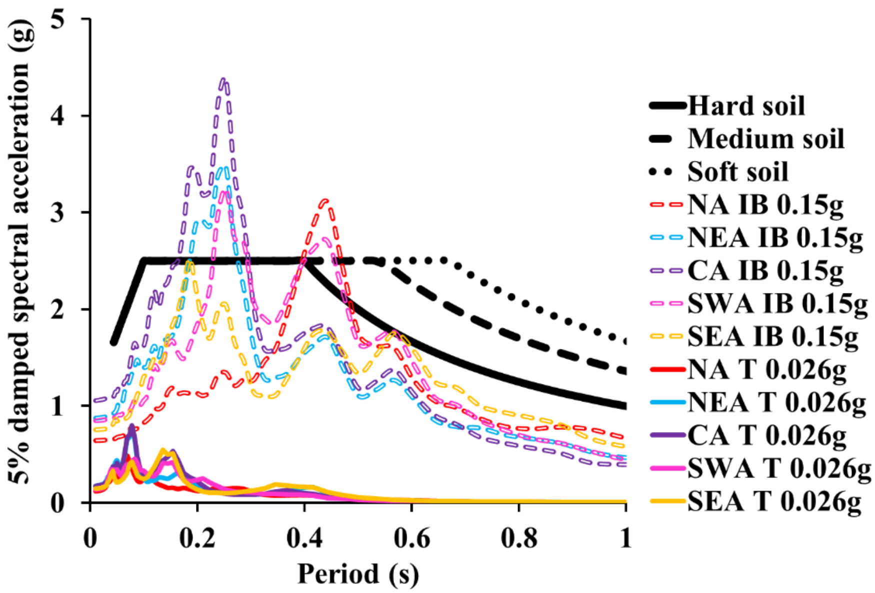

Fig. 17 Comparative of the 5% damped spectral accelerations at the surface averaged over the various zones of Itanagar city considering Tezpur (0.026g) and Indo-Burma (0.343g) earthquake motions

4.3 *Spatial variation of the spectral acceleration at different periods*

Figures 18-21 showcases the spatial variation on the 5% damped spectral acceleration at ground surface over the Itanagar city when subjected to strong motions of various energies. Specifically, the contours are highlighted for the periods of 0.1s, 0.3s, and 0.5s are chosen as they encompass the natural periods of single-story to standard 3-4 stories residential or commercial buildings (Anbazhagan and Sitharam 2008a; IS 1893 Part-1 2016). Furthermore, from Fig. 17, it can be noted that that the spectral accelerations in these periods exceed the codal recommendations for various types of soils (IS 1893 Part-1 2016) in the Itanagar region.

When subjected to 0.026g Tezpur motion, as shown in Fig. 18, at a period of 0.1 s, RKMH site exhibits the highest SA of 0.421g, thereby indicating significant seismic amplification for short-period structures such as single-story buildings. Conversely, NG site shows the lowest SA of 0.107g, suggesting more stable ground conditions for such structures. For the 0.3 s period, which affects mid-rise buildings, CMH/MGP site shows the highest SA at 0.203g, while IGP site has the lowest SA at 0.030g, thereby indicating relatively less amplification. At the 0.5 s period, relevant for relatively taller buildings, MOWB-II site records the highest SA at 0.128g, while DIV4 site shows the lowest SA at 0.020g, thereby reflecting the least amplification.

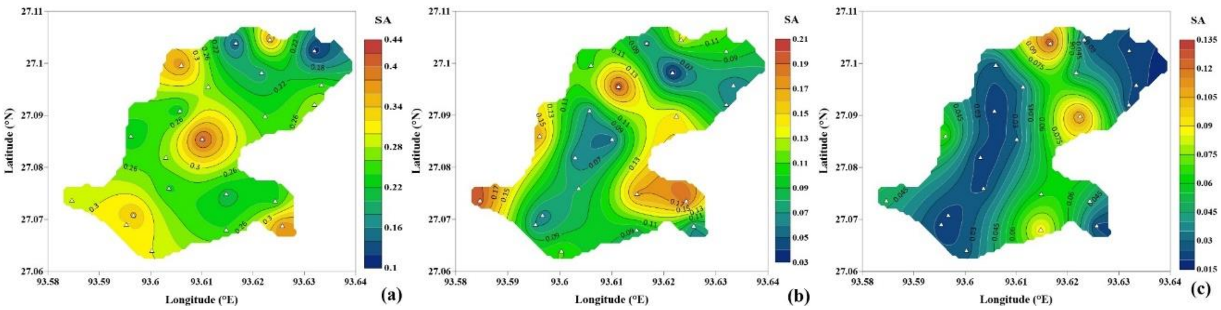

Fig. 18 Spatial variability of 5% damped spectral acceleration at Itanagar region when subjected to 0.026g Tezpur motion (a) 0.1s (b) 0.3s and (c) 0.5s

Figure 19 shows the spectral variation in the region when subjected to 0.15 Sikkim motion. As earlier, substantial seismic amplification for short-period structures is realized in the RKMH site as it exhibits the highest SA value of 2.984g at the 0.1 s period. In contrast, the MOWB-II site shows the lowest SA value of 0.384g. At the 0.3 s period, the BSI site has the highest SA of 2.534g, indicating significant amplification for mid-rise buildings, while the CVS site exhibited the lowest SA of 0.314g. For the 0.5s period, the DPSI site shows the highest SA value of 0.925g, while the IGP site has the lowest SA of 0.279g.

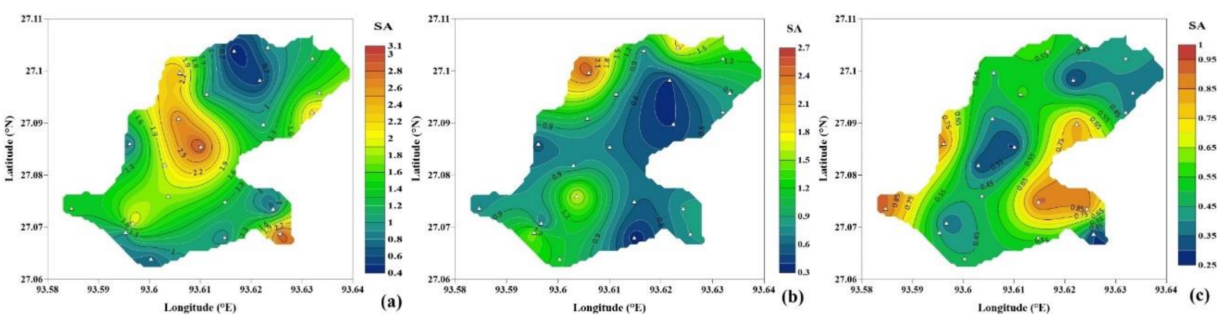

Fig. 19 Spatial variability of 5% damped spectral acceleration at Itanagar region when subjected to 0.15g Sikkim motion (a) 0.1s (b) 0.3s and (c) 0.5s

With the increase in the PBA of the strong motion, more and more region comes under the purview of increased seismic susceptibility. When subjected to the 0.343g Indo-Burma seismic motion, Figure 20 exhibits that for 0.1 s, 0.3 s and 0.5 s periods, the maximum spectral accelerations are noted at the JGG (2.892g), DNGC (4.09g) and BSI

(3.085g) sites respectively, while the IGP (0.286g), CVS (0.429g) and IGP (0.458g) sites, respectively, exhibited the lowest spectral acceleration values. Furthermore, when subjected to the 0.82g Kobe motion, Figure 21 exhibits that for 0.1 s, 0.3 s and 0.5 s periods, the maximum spectral accelerations are noted at the JGG (2.713g), DPH (5.341g) and DIV4 (7.110g) sites respectively, while the CVS site exhibited lowest spectral acceleration magnitudes (0.344g, 0.441g and 0.528g, respectively,) for all periods.

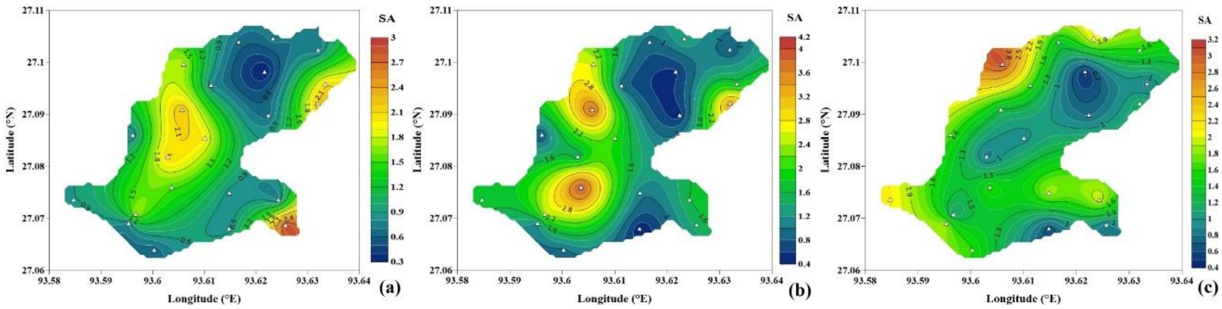

Fig. 20 Spatial variability of 5% damped spectral acceleration at Itanagar region when subjected to 0.343g Indo-Burma motion (a) 0.1s (b) 0.3s and (c) 0.5s

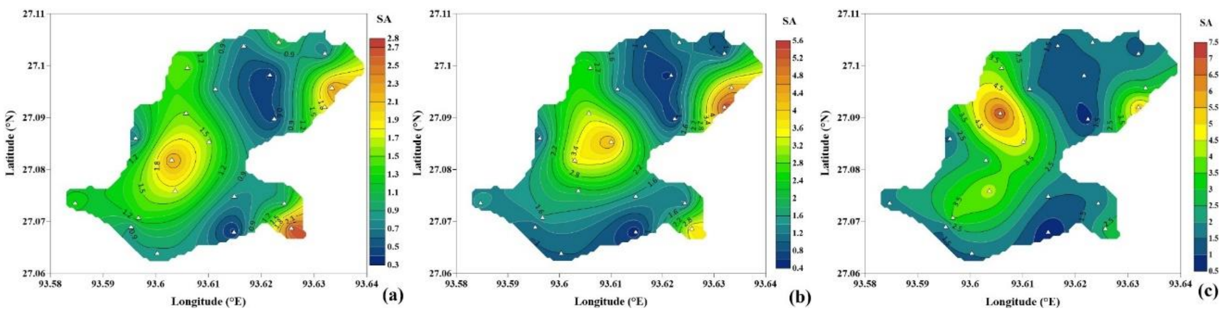

Fig. 21 Spatial variability of 5% damped spectral acceleration at Itanagar region when subjected to 0.82g Kobe motion (a) 0.1s (b) 0.3s and (c) 0.5s

In a nutshell, based on the strong motions chosen with a wide range of PBA (0.026g-0.82g), the findings from the ELGRA conducted in the urban areas of Itanagar reveal city that the seismic response is significantly influenced by the geological characteristics and variability of soil in the region. This analysis, which is the first of its kind for Itanagar, provides critical insights into the amplification factors and spectral accelerations that can guide the design of earthquake-resistant structures, particularly in light of the region's seismic history and the potential for future earthquakes. In this site response study, peak spectral acceleration (PSA) and the period corresponding to PSA for each location have been computed. This information is crucial from a design perspective, especially for accommodating buildings of varying heights in different regions. By understanding the PSA and its associated period, structural designs can be optimized for both short and tall buildings according to the potentiality of the damages to buildings of various heights, thereby incorpoating and enhancing their seismic resilience and compliance with building codes. The variation in SA across different sites underscores the importance of local site conditions in influencing seismic response and the necessity for site-specific seismic assessments to ensure earthquake-resistant designs.

7. Conclusions

1D equivalent linear ground response analysis (ELGRA) was carried out at 22 selected locations in Itanagar region using the DEEPSOIL commercial program. Four acceleration time histories with a wide range of PBA (0.026 Tezpur motion, 0.15 Sikkim motion, 0.343 Indo-Burma motion and 0.82 Kobe motion) were chosen to represent low, moderate, high and very high seismic hazards. The responses are strongly influenced not only by the local site geologies, but by the strong motion characteristics as well. Based on the analysis, the following conclusions are drawn.

- For any site, each of the ground response analysis parameters, i.e. profiles of ground acceleration, displacement, percentage strain and shear stress ratio increases with the PBA of the input strong motion. For peak bedrock accelerations of 0.026g, 0.15g, 0.343g and 0.82g, the surface-level accelerations over the Itanagar city spanned within 0.064g-0.290g, 0.236g-1.127g, 0.247g-1.328g and 0.32g-1.71g, respectively.
- The ELGRA response parameters have been averaged over the demarcated zones (NA, NEA, CA, SWA and SEA) to understand the zonal responses to strong motions. Although the overall displacement response of various zones does not exhibit significant difference under a particular strong motion, yet the magnitude and distributions of strain with depth vary significantly with the change in input strong motions. Such variations in strain significantly affect the development of damping at different layers of soil and eventually affect the surface level amplification of strong motion applied at the bottom of the profile.
- On an average, the Central and North-Eastern area of Itanagar city shows higher shear stress ratios than the other regions. The zone-wise shear stress ratio profiles indicate that only under very severe motions (PBA ≈ 0.82g), there is a possibility of loss of bearing and enhanced soil-structure interaction scenarios that demands additional attention when the typology of infrastructures are to be decided for the Central area of Itanagar. The rest of study area is found to be quite safe against any significant detrimental seismic hazard.
- It is observed that parts of North-Eastern (IF), South-Eastern (JGG), Central (RKMH, AS) as well as South-Western (DNGC, KV2) areas of Itanagar city exhibit significant amplification. With the increase in the PBA of the input strong motion, there is an increase in the strain induced in the system. As damping increases with induced strain, the surface level amplification of the acceleration decreases. Accordingly, for PBAs of 0.026g, 0.15g, 0.343g and 0.82g, the surface-level amplification factors over the Itanagar city span within 1.5-11, 1.57-7.51, 0.72-3.87 and 0.4-2.1. It can be noted that not only the amplification factor decreases with the increase in the PBA, the range over which it spans also narrows down. For few specific sites namely, IGP, CVS, GHSS, GSIC, MOWB-II, DPS, CMH/MGP and SLSA, deamplification is noted when subjected higher PBA motions such as the Indo-Burma and Kobe earthquakes. Engineers can use these ranges and magnitudes of AFs to predict the response of different buildings at higher levels of seismic activity, ensuring more consistent safety standards in areas prone to earthquakes. Furthermore, by understanding the narrowing AF range, the engineers can optimize materials and construction techniques for maximum resilience of upcoming infrastructure.

- The peak spectral acceleration (PSA) values derived from ground response analysis in Itanagar city show significant spatial variation when subjected to strong motions with varying PBAs. In comparison to the others, sufficiently high magnitudes of spectral acceleration are exhibited by the DIV4, RKMH, JGG, DPH, AS, IF, DNGC, KV2 and BSI sites, thereby attracting more seismic forces in case of an earthquake event and demanding more attention from seismic design and resilience of existing and upcoming infrastructures.
- The peak spectral acceleration magnitudes are also largely affected by the PBA of the input motion. With the increase in the PBA, expectedly, an increment is recorded in the peak spectral acceleration magnitudes averaged over each zone of Itanagar city. With the change in PBA, the period bandwidth of PSA also changes. When subjected to 0.026g Tezpur motion, the period bandwidth of PSA occurrence is found to be 0.05-0.2 s, while the same was determined to be 0.2-0.4 s when subjected to 0.343 Indo-Burma motion.
- For the higher PBA Indo-Burma motion, the PSA in the Central, South-Western and some parts of North-Eastern areas of Itanagar city is found to exceed the national codal provisions of PSA, thereby exhibiting the vulnerability of the above stated zones of Itanagar city to earthquakes within the periods of 0.2-0.4 s. These are critical observations for engineering and design purposes, as structures with natural periods in this range may experience significant seismic forces when subjected to higher PBA motions.
- Spatial variation of spectral acceleration at various periods provided the potential vulnerability of buildings of different heights around the Itanagar city. At the RKMH and JGG sites, the low-rise buildings with natural period around 0.1 s would be subjected to significant spectral accelerations. Similarly, the mid-rise buildings with natural period approximately 0.3 s and located at the CMH/MGP, BSI, DNGC and DPH would manifest significant spectral accelerations. The taller buildings with natural periods around 0.5 s would be under the radar of high spectral accelerations if located in the sites of MOWB-II, DPSI, BSI and DIV4. These findings would provide a guideline to the practicing professionals deciding for the height and corresponding period of the upcoming infrastructure in these areas. For existing infrastructure, this information could be used to act upon the mass and stiffness of the structures of specific heights to alter their natural periods to draw the infrastructure away from their potential vulnerability.

The analyses highlight the critical role of site-specific geological conditions and the incumbent strong motion in influencing the seismic response of the Itanagar region. While this study primarily focuses on site response, the findings can serve as a foundation for future research on seismic retrofitting strategies, including structural reinforcement and foundation improvement techniques. Implementing site-specific retrofitting measures based on these results could enhance the seismic resilience of structures in Itanagar. The observations and results provide valuable insights for engineers and planners, facilitating the development of more resilient structures that can withstand the unique seismic challenges posed by the diverse soil types prevalent in the region. Future research should focus on developing the seismic microzonation of the Itanagar city and look forward to integrating these findings into broader seismic risk management frameworks in enhancing preparedness and response strategies in earthquake-prone areas. Further, conducting soil-structure interaction (SSI) studies based on the findings from GRA remain critical for assessing seismic risk in urban areas and that its inclusion can improve the applicability of the study to infrastructure resilience planning. ELGRA provides immense information on the ground motions generated at different levels in the soil, which can be used in SSI studies (whether in lumped parameter or in continuum approaches) for defining the mechanical properties or interaction parameters to address the stress transfers between the substructure footing and the foundation soil. Such studies, in line of that available in previous literature (Sharma *et al.* 2018; Sharma *et al.* 2020; Sharma *et al.* 2021; Sharma *et al.* 2022; Sharma *et al.* 2023), can be conducted for the Itanagar region in future.

Compliance with Ethical Standards

Conflict of Interest: On behalf of all authors, the corresponding author declares that there are no conflicts of interest.

Ethical Approval: This article does not include any studies involving human participants or animals conducted by any of the authors.

Informed Consent: For this type of study, formal consent is not required.

Author Contributions: AKA: Formal analysis, Writing – Original preparation; AD: Conceptualization, Writing – Original preparation, Revision and Editing of drafted manuscript; SK: Revision and Editing of drafted manuscript; JT: Supervision, Formal analysis, Revision and Editing of drafted manuscript.

Funding: The authors thank the Arunachal Pradesh Public Work Department for funding the project "Seismic microzonation of Itanagar region" (Ref.No. CE/P/JT/02/2022/PWD).

References

Al-Asadi, Ali K, Alrebeh S 2024 Seismic resilience: Innovations in structural engineering for earthquake-prone areas. *Open Eng.* 14:1-11, https://doi.org/10.1515/eng-2024-0004.

Anbazhagan P, Kumar A, Sitharam TG 2013 Seismic site classification and empirical correlation between standard penetration test N-value and shear wave velocity for deep soil sites in Indo-Gangetic Basin. *Pure Appl. Geophy.* 170(3): 299-318, https://doi.org/10.1007/s00024-012-0525-1.

Anbazhagan P, Sitharam TG 2008 Seismic microzonation of Bangalore. *J. Earth Sys. Sci.* 117(S2): 833–52 https://doi.org/10.1007/s12040-008-0071-5.

Anbazhagan P, Sitharam TG 2008a Site characterization and site response studies using shear wave velocity. *J. Seism. Earthq. Eng.* 10(2), 53-67.

Anshu AK, Taipodia J, Kumar SS, Dey A 2024 Identification of ground response parameters of Itanagar city, Arunachal Pradesh, India, using varying seismic intensities and equivalent linear analysis approach. *Ind. Geotec h. J.* 1-23, https://doi.org/10.1007/s40098-024-00967-w.

Assimaki D, Kausel E 2002 An equivalent linear algorithm with frequency- and pressure-dependent moduli and damping for the seismic analysis of deep sites. *Soil Dyn. Earthq. Eng.* 22:959-965, https://doi.org/10.1016/S0267-7261(02)00120-3.

Baglari D, Dey A, Taipodia J 2020 A critical insight into the influence of data acquisition parameters on the dispersion imaging in passive roadside MASW survey. *J. App. Geophys.* 183(104223):1-20, https://doi.org/10.1016/j.jappgeo.2020.104223.

Banerjee R, Bandyopadhyay S, Singh T, Sengupta A, Reddy G R, Coleman J, Bolisetti C 2020 An in-house code for studying the response of soil deposits in Mumbai city using 2-D equivalent linear and 1-D nonlinear approach. *Geomech. Geoeng.* 17(1): 220–245, https://doi.org/10.1080/17486025.2020.1728395.

Bansal BK, Vandana C 2007 Microzonation Studies in India: DST initiatives I, *Proceedings on the Works on Microzonation*, Indian Institute of Science Bangalore, 1-6.

Basu D, Dey A 2016 Comparative 1D ground response analysis of homogeneous sandy stratum using linear, equivalent linear and nonlinear Masing approaches. *Nat. Sem. Geotech. Infrastr. Dev.* Kolkata, India, 1-7.

Basu D, Dey A, Kumar SS 2017 One-dimensional effective stress non-Masing nonlinear ground response analysis of IIT Guwahati. *Int. J. Geotech. Earthq. Eng.* 8(1):1-27, https://doi.org/10.4018/IJGEE.2017010101.

Basu D, Madhulatha B, Dey A 2019 A time-domain nonlinear effective-stress non-masing approach of ground response analysis of Guwahati city, India. *Earthq. Eng. Eng. Vib.* 18:61-75, https://doi.org/10.1007/s11803-019-0490-0.

Bilham R., 2019 Himalayan earthquakes: A review of historical seismicity and early 21st century slip potential. *Geological Society, London, Special Publications*. 483(1), 423-482.

Boominathan A, Dodagoudar GR, Suganthi A, Maheshwari RU 2008 Seismic hazard assessment of Chennai city considering local site effects. *J. Earth Sys. Sc.* 117(2):853-863, https://doi.org/10.1007/s12040-008-0072-4.

Bouckovalas GD, Papadimitriou AG 2005 Numerical evaluation of slope topography effects on seismic ground motion. *Soil Dyn. Earthq. Eng.* 25:547-558, https://doi.org/10.1016/j.soildyn.2004.11.008.

Choudhury D, Savoikar P 2009 Equivalent linear seismic analysis of MSW landfills using DEEPSOIL. *Eng. Geol.* 107(3-4):98-108, https://doi.org/10.1016/j.enggeo.2009.05.004.

Debnath A, Taral S, Mullick S, Chakraborty T 2021 The Neogene Siwalik succession of the Arunachal Himalaya: A revised lithostratigraphic classification and its implications for the regional paleogeography. *J. Geol. Soc. India* 97(4):339-350, https://doi.org/10.1007/s12594-021-1692-4.

Dey A, Kumar SS, Krishna, AM 2021 Nonlinear Ground Response Analysis: A Case Study of Amingaon, North Guwahati, Assam. *Lat. Dev. Geotech. Earthq. Eng. Soil Dyn*. 539-550, https://doi.org/10.1007/978-981-16-1468-2_28.

Fayjaloun R, Negulescu C, Roullé A, Auclair S, Gehl P, Faravelli M 2021 Sensitivity of earthquake damage estimation to the input data (Soil Characterization Maps and Building Exposure): Case study in the Luchon Valley, France. *Geosc.* 11(6):249, https://doi.org/10.3390/geosciences11060249.

Foti S, Hollender F, Garofalo F, Albarello D, Asten M, Bard C, Socco V et al. 2018 Guidelines for the good practice of surface wave analysis: a product of the Inter PACIFIC project. *Bull. Earthq. Eng*. 16, 2367-2420.

Gazetas G 1982 Vibrational characteristics of soil deposits with variable wave velocity. *Int. J. Num. Ana. Meth. Geomech.* 6:1-20, https://doi.org/10.1002/nag.1610060103.

Gazetas G 1991 Formulas and charts for impedances of surface and embedded foundations. *J. Geotech. Eng. ASCE* 117(9):1363-1381, https://doi.org/10.1061/(ASCE)0733-9410(1991)117:9(1363).

Govindaraju L, Ramana GV, Hanumantha Rao C, Sitharam TG 2004 Site-specific ground response analysis. *Current Sci.* 87(10): 1354-1362.

Guzel Y, Rouainia M, Elia G 2020 Effect of soil variability on nonlinear site response predictions: Application to the Lotung site. *Comp. Geotech.* 121:103444, https://doi.org/10.1016/j.compgeo.2020.103444.

Hashash YM, Musgrove MI, Harmon JA, Groholski DR, Phillips CA, Park D 2024 DEEPSOIL 7.1, user manual. Urbana, IL, Board of Trustees of University of Illinois at Urbana-Champaign.

https://www.itanagarsmartcity.org/ (Last accessed: 09.10.2024).

Idriss IM, Sun JI 1992 SHAKE91: A computer program for conducting EQL seismic response analyses of horizontally layered soil deposits. Center for Geotechnical Modeling, University of California, US.

IS 1893 Part-1 2016 Criteria for earthquake resistant design of structures-general provision and buildings. (Sixth Revision), Bureau of Indian Standards, New Delhi.

Jiang C, Yahong D, Huangdong M, You X, Ge C 2022 A microtremor study to reveal the dynamic response of earth fissure site: the case study in Fenwei Basins, China. *Env. Earth Sci.* 81(3), https://doi.org/10.1007/s12665-022-10217-y.

Kaklamanos J, Baise LG, Boore DM 2011 Estimating unknown input parameters when implementing the NGA ground-motion prediction equations in engineering practice. *Earthq. Spectra*. 27:1219–1235, https://doi.org/10.1193/1.3650372.

Kaklamanos J, Bradley BA, Thompson EM, Baise LG 2013 Critical parameters affecting bias and variability in site-response analyses using KiK-net downhole array data. *Bull. Seism. Soc. America*. 103:1733-1749, https://doi.org/10.1785/0120120166.

Kanli AI 2010 Integrated approach for surface wave analysis from near-surface to bedrock. *Advances in Near-Surface Seismology and Ground-Penetrating Radar*, Geophysical Developments Series No. 15, *SEG Reference Publications*. 29, 461-476. 10.1190/1.9781560802259.ch29

Kanli AI, Kang TS, Pinar A, Tildy P, Prónay Z 2008 A systematic geophysical approach for site response of the Dinar region, Southwestern Turkey. *J. Earthq. Eng*. 12(S2), 165-174. https://doi.org/10.1080/13632460802013966

Kanli AI, Tildy P, Prónay Z, Pınar A, Hermann L 2006 V_S^{30} mapping and soil classification for seismic site effect evaluation in Dinar region, SW Turkey. *Geophysical J. Int.* 165(1), 223-235. https://doi.org/10.1111/j.1365-246X.2006.02882.x

Khan MY, Turab SA, Ali L, Shah MT, Qadri ST, Latif K, Kanli AI, Akhter MG 2021 The dynamic response of coseismic liquefaction-induced ruptures associated with the 2019 M w 5.8 Mirpur, Pakistan, earthquake using HVSR measurements. *The Lead. Edge*. 40(8), 590-600, https://doi.org/10.1190/tle40080590.1.

Kim B, Hashash YMA, Stewart JP, Rathje EM, Harmon JA, Musgrove MI, Campbell KW, Silva WJ 2016 Relative differences between nonlinear and equivalent-linear 1-D site response analyses. *Earthq. Spectra.* 32:1845–1865, https://doi.org/10.1193/051215eqs068m.

Kramer SL 1996 Geotechnical Earthquake Engineering. Prentice Hall, New York.

Kumar A, Anbazhagan P, Sitharam T G 2013 Seismic hazard analysis of Lucknow considering local and active seismic gaps. *Nat. Haz.* 69:327-350, https://doi.org/10.1007/s11069-013-0712-0.

Kumar P, Kumar SS 2023 Development of synthetic acceleration time histories for seismic ground response studies for site classes C to E for Bihar region: a case study. *Inn. Infrastr. Sol.* 8:292, https://doi.org/10.1007/s41062-023-01265-9.

Kumar SS, Dey A, Krishna AM 2018 Importance of site-specific dynamic soil properties for seismic ground response studies: Ground response analysis. *Int. J. Geotech. Earthq. Eng*. 9(1):78-98, https://doi.org/10.4018/IJGEE.2018010105.

Kumar SS, Dey A, Krishna AM 2020 Monotonic and dynamic properties of riverbed sand and hill-slope soils of seismically active North-east India for ground engineering applications. *Int. J. Geo-Eng*. 11:1-21, https://doi.org/10.1186/s40703-020-00116-1.

Kumar SS, Murali Krishna A, Dey A 2014 Equivalent linear and nonlinear ground response analysis of two typical sites at Guwahati city. *Ind. Geotech. Conf.* Kakinada, India, 603-612.

Lee SHH 1992 Analysis of the multicollinearity of regression equations of shear wave velocities. *Soils Found.* 32(1): 205–214, https://doi.org/10.3208/sandf1972.32.205.

Mahajan AK, Sporry RJ, Champati Ray PK, Ranjan R, Slob S, Van WC 2007 Methodology for site-response studies using multi-channel analysis of surface wave technique in Dehradun city. *Current Sci.* 92(7): 945-955, http://www.jstor.org/stable/24097675.

Maheswari RU, Boominathan A, Dodagoudar GR 2008 Nonlinear seismic response analysis of selected sites in Chennai. *Proc. 12th Int. Conf. Int. Assoc. Comp. Meth. Advan. Geomech.* India, 2835- 2842.

Maheswari RU, Boominathan A, Dodagoudar GR 2010 Seismic site classification and site period mapping of Chennai City using geophysical and geotechnical data. *J. App. Geophys.* 72(3):52-168, https://doi.org/10.1016/j.jappgeo.2010.08.002.

Mhaske SY, Choudhury D 2011 Geospatial contour mapping of shear wave velocity for Mumbai city. *Nat. Haz.* 59:317-327, https://doi.org/10.1007/s11069-011-9758-z.

Mohan K, Dugar S, Pancholi V, Dwivedi VK, Kumar N, Sairam B, Chopra S 2024 A multi-scenario based micro seismic hazard assessment of the Bhuj City, western India incorporating geophysical and geotechnical parameters. *Quat. Sc. Adv.* 13:100138-1-23, https://doi.org/10.1016/j.qsa.2023.100138.

Mullick S, Sinha S 2024 Evidence of fluvial to marine transition in the Siwalik rocks of the Itanagar area, Arunachal Pradesh, India: Implication for the regional paleogeography. *Him. Geol.* 45(1):138-154.

Naik N, Choudhury D (2013) Site specific ground response analysis for typical sites in Panjim city, Goa. *Proc. Ind. Geotech. Conf.* Roorkee, India, 1-10.

Nath SK, Thingbaijam KKS, Raj A 2009 Earthquake hazard in North-East India: A seismic microzonation approach with typical case studies from Sikkim Himalaya and Guwahati city. *J. Earth Sys. Sci.* 117(S2):809-831, https://doi.org/10.1007/s12040-008-0070-6.

NEHRP 2020 NEHRP recommended provisions for seismic regulations for new buildings and other structures - Part I: Provisions and Part II: Commentary. FEMA P-2082-1, *Fed. Emerg. Management Auth. BSSC*, National Institute of Building Sciences, Washington D.C.

Ordonez GA 2011 Shake 2000: A computer program for the 1D analysis of geotechnical earthquake engineering. *2nd Revision*.

Park C B, Miller R D, Xia J 1999 Multichannel analysis of surface waves. *Geophys.* 64(3):800-808, https://doi.org/10.1190/1.1444590.

Phanikanth VS., Choudhury D, Reddy G R 2011 Equivalent-linear seismic ground response analysis of some typical sites in Mumbai. *Geotech. Geol. Eng.* 29(6): 1109-1126, https://doi.org/10.1007/s10706-011-9443-8.

Pitilakis D, Clouteau D 2010 Equivalent linear substructure approximation of soil-foundation-structure interaction: Model presentation and validation. *Bull. Earthq. Eng.* 8:257-282, https://doi.org/10.1007/s10518-009-9128-3.

Puri N, Jain A, Mohanty P, Bhattacharya S 2018 Earthquake response analysis of sites in state of Haryana using DEEPSOIL software. *Proc. Comp. Sci*. 125:357-366, https://doi.org/10.1016/j.procs.2017.12.047.

Rao KS, Rathod GW 2014 Seismic microzonation of Indian megacities: A case study of NCR Delhi. Ind. Geotech. J. 44:132–148, https://doi.org/10.1007/s40098-013-0084-0.

Rao NP, Kumar MR, Seshunarayana T, Shukla AK, Suresh G, Pandey Y, Gupta H 2011 Site amplification studies towards seismic microzonation in Jabalpur urban area, Central India. *Phys. Chem. Earth* 36(16):1247-1258, https://doi.org/10.1016/j.pce.2011.01.002.

Rathje E, Pehlivan M, Gilbert R, Rodriguez-Marek A 2015 Incorporating site response into seismic hazard assessments for critical facilities: A probabilistic approach. *Perspectives on Earthquake Geotechnical Engineering: In Honour of Prof. Kenji Ishihara*, 93-111, https://doi.org/10.1007/978-3-319-10786-8_4.

Rathje EM, Kottke AR, Trent WL 2010 Influence of input motion and site property variabilities on seismic site response analysis. *J. Geotech. Geoenv. Eng. ASCE* 136(4):607–19, https://doi.org/10.1061/(ASCE)GT.1943-5606.0000255.

Reddy MM, Rao CH, Reddy KR 2022 Site-specific ground response analysis of some typical sites in Amaravati Region, Andhra Pradesh, India. *Ind. Geotech. J.* 52: 39–54, https://doi.org/10.1007/s40098-021-00562-3.

Sabetta F, Fiorentino G, Bocchi F 2023 Influence of local site effects on seismic risk maps and ranking of Italian municipalities. *Bull. Earthq. Eng.* 21: 2441–2468, https://doi.org/10.1007/s10518-023-01619-9.

Sairam B, Singh AP, Patel V, Pancholi V, Chopra S, Dwivedi VK, Kumar MR 2018 Influence of local site effects in the Ahmedabad mega city on the damage due to past earthquakes in northwestern India. *Bull. Seism. Soc. Am.* 108(4):2170-2182, https://doi.org/10.1785/0120170266.

Seed HB, Idriss IM 1970 Soil moduli and damping factors for dynamic response analysis. *Report No. EERC 70-10*, University of California, Berkeley, USA.

Seismosoft 2012 Seismosignal, version 5.0. Retrieved from www.seismosoft.com.

Sharma N, Dasgupta K and Dey A 2018 Seismic SSI effects on fundamental period of reinforced concrete frame with shear wall. *Proc. 11 Struc. Eng. Conv.*, Kolkata, India, 1-6.

Sharma N, Dasgupta K and Dey A 2020 Natural period of reinforced concrete building frames on pile foundation considering seismic soil structure interaction. *Structures* 27, 1594-1612, https://doi.org/10.1016/j.istruc.2020.07.010

Sharma N, Dasgupta K and Dey A 2021 Seismic behaviour of RC building frame subjected to soil-structure interaction effects. *Adv. Struc. Vib.: Sel. Proc. ICOVP 2017*, 157-170, https://link.springer.com/chapter/10.1007/978-981-15-5862-7_14

Sharma N, Dasgupta K and Dey A 2022 Prediction of natural period of RC frame with shear wall supported on soil-pile foundation system using Artificial Neural Network. *J. Earthq. Eng.* 26(8), 4147-4171, https://doi.org/10.1080/13632469.2020.1824876

Sharma N, Dasgupta K and Dey A 2023 Soil-structure interaction induced modification on the natural period of reinforced concrete buildings. *Proc. 2022 Eurasian OpenSees Days*, 352-361, https://link.springer.com/chapter/10.1007/978-3-031-30125-4_32

Stewart JP, Chiou S-J, Bray JD, Graves RW, Somerville PG, Abrahamson NA 2002 Ground motion evaluation procedures for performance-based design. *Soil Dyn. Earthq. Eng.* 22:765–772, https://doi.org/10.1016/s0267-7261(02)00097-0.

Taipodia J, Baglari D, Dey A 2018 Recommendations for generating dispersion images of optimal resolution from active MASW survey. *Inn. Infra. Sol. 3*:1-19, https://doi.org/10.1007/s41062-017-0120-5.

Taipodia J, Dey A 2017 Impact of frequency filtering and temporal muting on the resolution of dispersion image. *13th Int. Conf. Vib. Prob*. Guwahati, India, 1-11.

Taipodia J, Dey A, Baglari D 2018a Influence of signal preprocessing parameters on the resolution of dispersion image from active MASW survey. *J. Geophys. Eng*. 15(4): 1310-1326, https://doi.org/10.1088/1742-2140/aaaf4c.

Taipodia J, Dey A, Baglari D 2021 Influence of receiver layout on active MASW survey conducted at different sites having varying substrata characteristics. *Arab. J. Geosc*. 14(12):1143, https://doi.org/10.1007/s12517-021-07143-x.

Taipodia J, Madhulatha B, Dey A 2018b Influence of stacking on the resolution of the dispersion image in active MASW survey. *Ind. Geotech. Conf.* Bangalore, India, 1-8.

Taipodia J, Madhulatha B, Dey A, Acharyya R, Sarma CP 2020 1-D and 2-D active MASW survey for subsurface profiling of Jia Bharali river bed, Assam, India, for a proposed 1.2 km road bridge. *Prac. Period. Struc. Des. Cons. ASCE* 25(3): 05020008-1-15, https://doi.org/10.1061/(ASCE)SC.1943-5576.0000495.

Tallini M, Morana E, Guerriero V 2024 Seismic microzonation studies by using the equivalent linear approach (L'Aquila, Central Italy). *Proc. 18th World Conf. Earthq. Eng.* Milan, Italy, 1-10.

Tempa K, Chettri N, Gurung L 2021 Shear wave velocity profiling and ground response analysis in Phuentsholing, Bhutan. *Inn. Infrastr. Sol.* 6:78, https://doi.org/10.1007/s41062-020-00420-w.

Tsiapas YZ, Bouckovalas GD 2019 Equivalent linear computation of resposne spectra for liquifiable sites: The spectral interpolation method. *Soil Dyn. Earthq. Eng.* 116:541-551, https://doi.org/10.1016/j.soildyn.2018.10.033.

Wang G, Yuan M, Ma X, Wu J 2017 Numerical study on the seismic response of the underground subway station-surrounding soil mass-ground adjacent building system. *Front. Struct. Civ. Eng*. 11:424–435, https://doi.org/10.1007/s11709-016-0381-7.

Xia J, Miller RD, Park CB 1999 Estimation of near-surface shear-wave velocity by inversion of Rayleigh waves. *Geophys.* 64(3):691-700, https://doi.org/10.1190/1.1444578.

Xia J, Miller RD, Park CB, Hunter JA, Harris JB, Ivanov J 2002 Comparing shear-wave velocity profiles inverted from multichannel surface wave with borehole measurements. *Soil Dyn. Earthq. Eng*. 22(3), 181-190, https://doi.org/10.1016/S0267-7261(02)00008-8.

Yoshida N, Kobayashi S, Suetomi I, Miura K. 2002 Equivalent linear method considering frequency dependent characteristics of stiffness and damping. *Soil Dyn. Earthq. Eng.* 22:205-222, https://doi.org/10.1016/S0267-7261(02)00011-8.